

Dietary advanced glycation end-products promote food allergy by disrupting intestinal barrier and enhancing Th2 immunity

Received: 19 September 2024

Accepted: 19 May 2025

Published online: 28 May 2025

 Check for updates

Qiaozhi Zhang^{1,7}, Gang Yu^{1,7}, Yuhao Jiang¹, Haining Shi², Xiaorong Yang³, Zhongshan Gao⁴, Qingqing Wang⁵, Jinlu Sun⁶, Chong Wang¹, Qianqian Li¹, Huatao Li¹ & Linglin Fu¹✉

Epidemiological studies have suggested a link between the consumption of foods high in advanced glycation end-products (AGEs) and an increased risk of food allergy (FA). However, the underlying mechanisms remain largely unelucidated. In this study, we present complementary epidemiological and experimental evidence showing the pathogenic role of dietary AGEs (dAGEs) in facilitating the development of FA. We first provide a population-based cross-sectional survey supporting the association between a dietary pattern rich in AGE-laden processed foods and an increased prevalence of self-reported allergic diseases, including FA. Through multiple experimental models of FA, we demonstrate that exposure to dAGEs promotes susceptibility to allergic sensitization and amplifies Th2-biased immune response to concomitant food allergens. dAGEs possess both barrier-disruptive and Th2-adjuvant properties to induce a compromised intestinal barrier function and Th2-skewed immunity at intestinal mucosal sites. This aberrant immune response is mediated by the intricate interplay between the receptor for AGEs (RAGE) and toll-like receptor-4 (TLR4) signaling pathways. Furthermore, the Th2-stimulating effect of dAGEs involving RAGE-TLR4 crosstalk was validated in human peripheral immune cells. This study contributes to our understanding of dAGEs as a risk factor for FA and highlights the potential of dAGEs restriction as a promising preventative strategy for susceptible populations.

Epidemiologic studies have witnessed a continuous rise in the incidence and severity of food allergy (FA) worldwide, especially in westernized countries, with cow's milk and eggs being the most prevalent allergens in most regions^{1–3}. An in-depth understanding of the pathogenesis of FA is essential for developing effective therapeutic strategies. Given that genetic predisposition is not sufficient to explain the recent surge in allergic conditions in many areas, environmental

factors associated with modern lifestyles, particularly dietary habits, have been raised as important drivers behind this epidemiologic trend^{4,5}. This is further supported by migration studies showing that individuals who move to high-prevalence regions, especially during early childhood, experience increased allergy risks, underscoring the important role of environmental exposures during critical windows in allergy development⁶.

¹School of Food Science and Biotechnology, Zhejiang Gongshang University, Hangzhou 310018, PR China. ²Mucosal Immunology and Biology Research Center, Harvard Medical School, Boston, MA 02129, USA. ³School of Statistics and Mathematics, Zhejiang Gongshang University, Hangzhou 310018, PR China. ⁴Allergy Research Center, Zhejiang University, Hangzhou 310018, PR China. ⁵Institute of Immunology, Zhejiang University School of Medicine, Hangzhou 310058, PR China. ⁶Allergy Department, State Key Laboratory of Complex Severe and Rare Diseases, Peking Union Medical College Hospital, 100730 Beijing, PR China. ⁷These authors contributed equally: Qiaozhi Zhang, Gang Yu. ✉e-mail: fulinglin@zjgsu.edu.cn

A key hallmark of the modern diet is overindulged in refined ingredients and highly processed foods. Ultra-processed foods (UPFs) are ready-to-eat formulations of food ingredients made mostly from industrial techniques and processes with the addition of flavorings, colorings, texturizers, and other additives⁷. In the past few decades, UPFs has been dominating the food supply in high-income countries, and their consumption is rapidly increasing in middle-income countries as well⁸. Emerging evidence suggest that exposure to UPFs may exert detrimental effects on human health and contribute to the development of chronic non-communicable diseases, including allergies^{9–11}. One of the increasingly recognized and potentially harmful components of UPFs are advanced glycation end-products (AGEs)¹². Dietary AGEs (dAGEs) are a group of heterogeneous compounds formed primarily via the Maillard reaction between reducing sugars and amino groups in proteins or peptides within food matrices, as well as through lipid peroxidation and other oxidative pathways¹³. These compounds are generated during thermal processing of foods and are present in high levels in processed and cooked foodstuffs, especially those subjected to extensively heat treatments (e.g., grilled meats, fried foods and baked goods)^{14,15}. Common dAGEs include ϵ -(carboxymethyl)-lysine (CML) and methylglyoxal-derived hydroimidazolone isomers (MG-Hs), which can be quantified in foods using fluorescence spectroscopy or LC-MS/MS¹⁵. Long-term consumption of dAGEs was documented to accelerate the biological level of AGEs¹⁶. Once digested, dAGEs can be partially absorbed and accumulate within the body. An excessive level of biological AGEs was reported to stimulate oxidative stress and inflammation, at least in part, through their interaction with the receptor for AGEs (RAGE) present on cell surfaces¹⁷. Meanwhile, the unabsorbed dAGEs can reach the colon and metabolized by the gut microbiota, potentially leading to microbial dysbiosis and metabolic disorders that are involved in the pathogenesis of host immune disorders^{18–20}.

Recent research has implicated an adverse impact of dAGEs on gut homeostasis, manifested as mucosal damage, chronic inflammation and alterations in gut microbiota composition^{19–22}. These pathological changes may contribute to the development of FA by inducing gut barrier dysfunction, localized inflammation, and microbial dysbiosis—processes that are central to FA pathogenesis^{23,24}. Importantly, these AGE-induced alterations align with clinical observations of elevated AGE accumulation in the skin of FA patients²⁵ and epidemiological evidence linking high-AGE food consumption (e.g., fast food and fried/microwaved meat) with increased FA prevalence^{26–28}. However, to date, the precise mechanism by which dAGEs contribute to the pathogenic process of FA remains largely unknown. An in-depth understanding of the pathogenic role of dAGEs in FA would significantly enhance dietary intervention strategies for susceptible populations to prevent FA.

In this study, we first provided a population-based epidemiologic survey supporting that increased consumption of AGE-containing UPFs facilitated the risk of having allergic diseases, inclusive of FA. Subsequently, with multiple adjuvant-dependent and independent models of experimental FA, we show that exposure to dAGEs promoted the susceptibility of developing allergic reactions to bystander food allergens. This effect is mediated by the induction of a compromised intestinal barrier function, followed by Th2-skewed immune responses akin to mucosal adjuvants that involve the crosstalk between RAGE and toll-like receptor-4 (TLR4) signaling pathways. These findings highlight the significance of dAGEs as a risk factor for FA and underscore the importance of reducing dAGEs intake as a promising preventative strategy for populations at risk.

Results

Intake of AGE-containing UPFs is positively correlated with allergic diseases

As a considerable component of the modern and western diet, UPFs are recognized as a primary source of AGEs in the diet^{14,15}. We first

performed an epidemiologic study examining the relationship between UPFs intake and allergic outcomes based on the data from National Health and Nutrition Examination Survey (NHANES) during 2007–2010, a population-based, cross-sectional survey in the United States. During the NHANES cycles 2007–2010, self-reported atopic diseases, including FA, asthma and wheezing were assessed, along with detailed dietary intake records that allow us to investigate the associations between dietary factors and allergic disorders. General characteristics of the study participants ($n = 11,765$) stratified by quartiles of UPFs intake are presented in Supplementary Table S1. The study population included 4582 children (6–19 years) and 7183 adults (20–59 years). Participants with a higher consumption level of UPFs are more likely to be teenagers and young adults, and less likely to be individuals with a normal body mass index (BMI). Meanwhile, the prevalence of self-reported allergic diseases, including FA (from 7.7 to 9.3%, $p < 0.05$), asthma (from 14.5 to 18.5%, $p < 0.001$), and wheezing (from 11.6 to 13.8%, $p < 0.01$) was all found to be higher among persons with a higher preference for UPFs. Figure 1 summarizes the odds ratios (ORs) calculated for the associations between UPFs intake and allergic outcomes. Compared with participants in the lowest quartile of UPFs intake, those in the highest quartile had a significantly higher risk of having self-reported FA (95% confidence interval (CI), 1.02–1.47; p trend = 0.03), asthma (95% CI, 1.17–1.54; p trend < 0.001), and wheezing (95% CI, 1.05–1.42; p trend = 0.004) (Fig. 1, Model 1). This trend remains significant for FA and asthma after adjusting for several potential confounding factors, including dietary fiber, antioxidant intake and anthropometric parameters like BMI (Fig. 1, Models 2 and 3). We also observed increased ORs for increasing quartiles of UPFs intake associated with asthma symptoms, indicative of a dose-response trend. However, this trend was not observed for FA and wheezing, potentially due to threshold effects, population heterogeneity, or compounding factors. Overall, we present nationally-representative data suggesting that the consumption of AGE-containing UPFs is positively associated with an increased risk of self-reported allergic diseases, including FA.

Long-term exposure to dAGEs exacerbated allergic inflammation in rodent FA models

Having established the epidemiological correlation between intake of AGEs-rich foods and the incidence of FA, it is imperative to delve into the underlying immunological mechanisms. To explore the impact of dAGEs on FA risks, we fed BALB/c mice a thermally-processed diet or an isocaloric control diet for 12 weeks before induction of experimental FA (Fig. 2a). Heat processing of a standard chow diet (D12450H) is a well-validated method for preparing high-AGE diets^{18,20,22,29}, and expectedly, this treatment led to a 2.3-fold increase in the total AGEs content, including notable increases in the levels of prominent AGEs such as CML, N ϵ -carboxyethyllysine (CEL), and MG-Hs (Supplementary Fig. 2). Long-term exposure to dAGEs is well-documented to augment de novo accumulation of AGEs. As expected, feeding mice a high-AGE diet (HAGE) for 12 weeks resulted in 1.2 and 1.3-fold higher serum and fecal AGEs levels than that seen with the unheated control diet (SD; Fig. 2b and Supplementary Fig. 3a, b). After intragastrically challenged with ovalbumin (OVA, a major egg allergen), manifestations of food allergic responses were evident, as characterized by the increases in clinical allergy score and heightened levels of serum total and allergen specific antibodies. In contrast to sensitized mice fed SD, only sensitized mice fed HAGE exhibited a significantly higher allergy score compared to the non-sensitized control, albeit without a concomitant rise in specific antibody levels (Fig. 2c–e). Furthermore, sensitized mice fed HAGE showed marked increases in mast cell expansion and degranulation within the intestinal tissue compared to the SD control (Fig. 2f, g and Supplementary Fig. 3c), suggesting enhanced mast cell activation. Intriguingly, feeding mice with HAGE alone without allergen sensitization but with only high-dose OVA challenges was sufficient to elicit both total IgE and antigen-specific IgG1 responses (HAGE vs. SD;

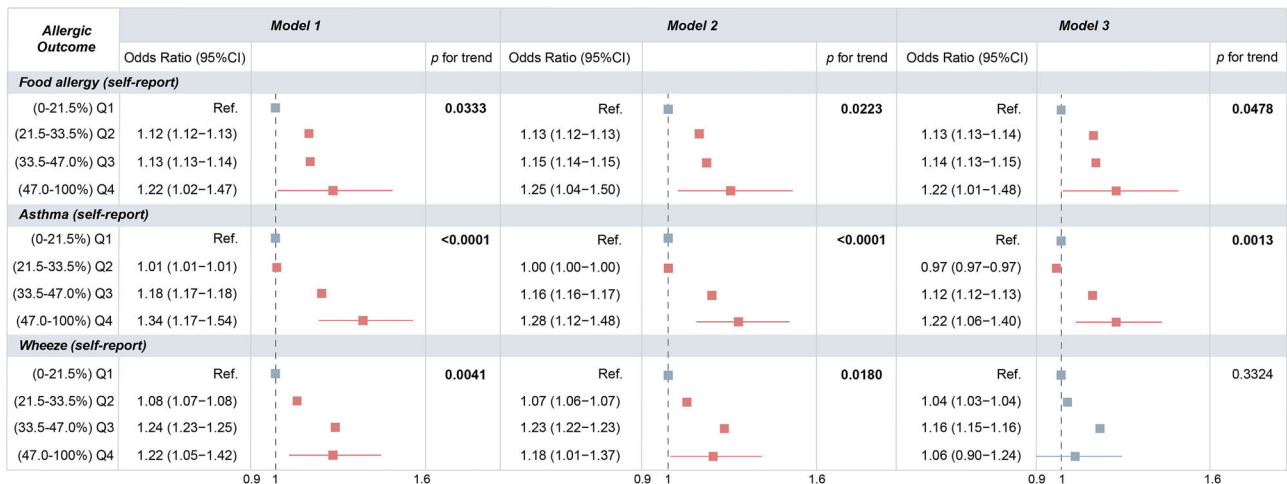


Fig. 1 | Forest plot showing odds ratios for UPFs intake and allergic disorders in NHANES 2007–2010. Model 1, adjusted for none. Model 2, adjusted for dietary fiber and CDAI. Model 3, adjusted for age, gender, race/ethnicity, educational level, BMI, dietary fiber and CDAI. $n = 11765$. p for trend (two-sided) was calculated by using the median value of each quartile as a continuous variable in each model. Data

represent odds ratios (center points) and their 95% CIs (error bars) derived from multivariable logistic regression analyses of allergic outcomes. Q1: the first quartile, et cetera. BMI body mass index, CDAI composite dietary antioxidant index, CI confidence interval, UPFs ultra-processed foods. Source data are provided as a Source Data file.

Fig. 2d, e). The expression level of mast cell proteases in the colon tissue was also higher in mice fed HAGE vs. SD control (HAGE vs. SD; Supplementary Fig. 3c). This suggest that prolonged consumption of a high-AGE diet induced allergic inflammatory responses, even after a few doses of antigen exposure. The HAGE diet likely exert an adjuvant-like effect, priming the immune system and enhancing its responsiveness to subsequently encountered allergens such as OVA. Mass cytometry (CyTOF) analysis of mesenteric lymph nodes (MLN) lymphocytes further revealed a higher proportion of Th2 cells in sensitized mice fed HAGE than that seen in sensitized mice fed SD (Fig. 2h, i). A lower frequency of Treg cells was also noted in HAGE-fed mice compared to SD-fed control in unsensitized groups. As a consequence, the secretory levels of Th1 cytokines (e.g., IFN- γ and IL-12) from MLN cells were markedly decreased in HAGE-fed mice relative to SD-fed control (Fig. 2j), manifesting a Th2-biased inflammatory response promoted by the consumption of dAGEs. In addition, we observed a higher proportion of NF- κ B⁺ cells in CD4⁺ T cells in HAGE-fed groups vs. SD-fed controls in association with the Th2-biased cytokine production (Fig. 2i, inset figure; Fig. 2j). This revealed a coordinated network of pro-inflammatory signaling in the regulation of T-helper cell effector function under a high-AGE diet.

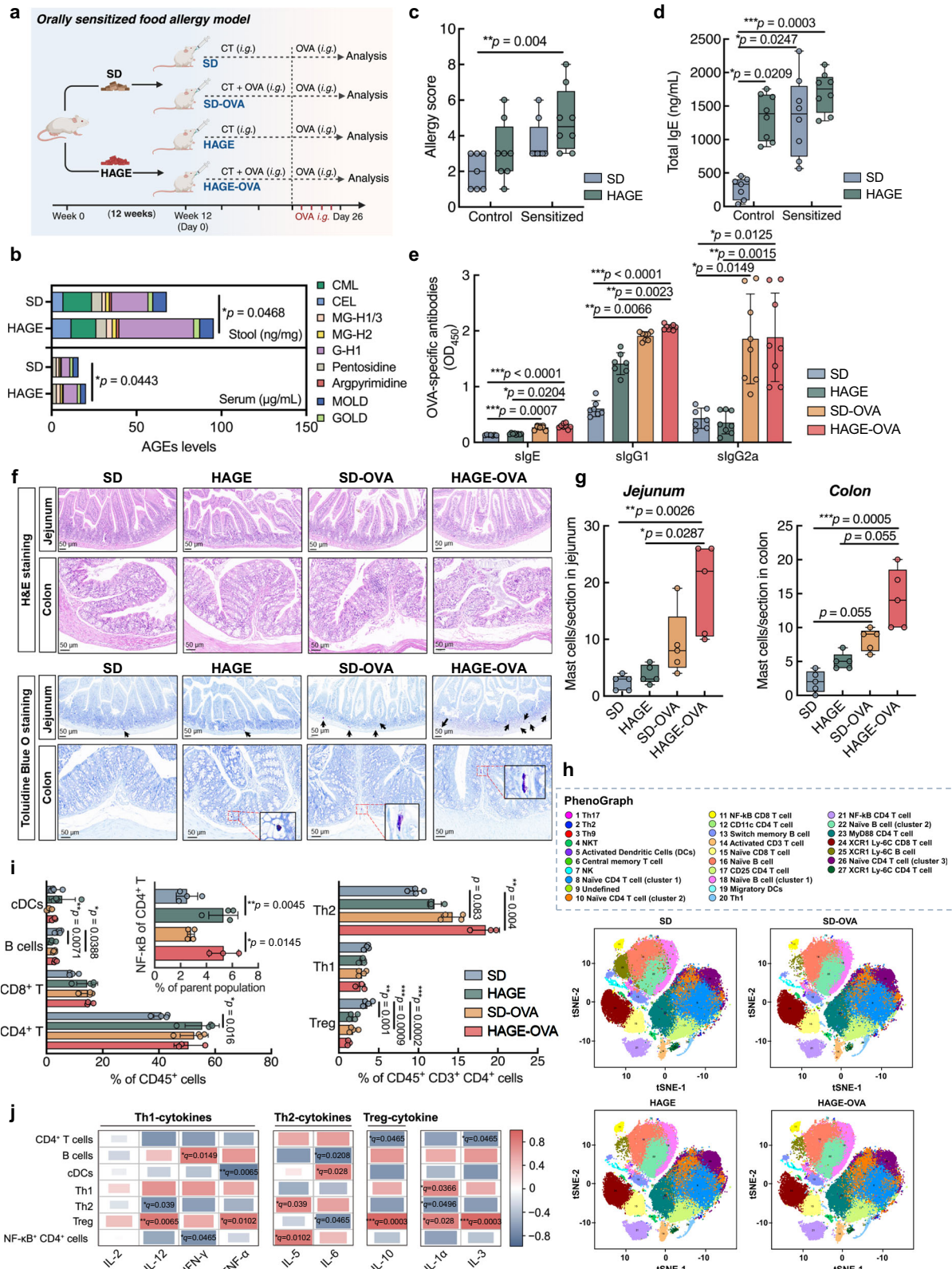
In parallel experiments, we established an epicutaneously sensitized FA model in C57BL/6j mice after a 12-week regimen of SD or HAGE (Supplementary Fig. 5a, b). Again, we noted accelerated de novo AGEs accumulation in HAGE-fed mice, especially in the feces (Supplementary Fig. 5c). Upon induction of experimental FA, HAGE-fed mice exhibited a trending severer ear thickness in concurrency with an approximately 1.9-fold increase in serum total IgE level relative to the SD control (Supplementary Fig. 5d–g). Histological evaluation of jejunum tissue evidenced a severer degree of intestinal mucosal injury in HAGE-fed mice compared to SD-fed control, similar to that observed in the orally sensitized model (Supplementary Fig. 5h). CyTOF analysis of lamina propria lymphocytes further pointed to an increased frequency of Th2 cells in sensitized mice fed HAGE relative to the SD control, along with a markedly higher proportion of effector cells including mast cells and basophils in the mucosa (Supplementary Fig. 6). Additionally, a higher frequency of TLR4⁺ and RAGE⁺ cells in CD45⁺ cells was also noted in HAGE-groups, indicative of heightened pro-inflammatory responses in lymphocytes under a high-AGE diet. Altogether, these results suggest that chronic exposure to a high-AGE diet exacerbates

allergic inflammation in multiple rodent models, potentially through mechanisms involving Th2 polarization driven by pro-inflammatory signaling pathways.

dAGEs intake induced intestinal barrier dysfunction and dysbiosis of the gut commensal consortium

An increased intestinal permeability and compromised mucosal barriers predispose to allergic and autoimmune disorders^{28,30}. We next questioned that whether dAGEs could act as barrier-damaging agents to induce intestinal barrier dysfunction that underly the onset of aberrant immune responses (Fig. 3a). Compared to SD-fed control, HAGE intake for 12 weeks induced intestinal permeabilization, as evidenced by an in vivo FITC-Dextran assay (Fig. 3b). This disrupted intestinal barrier integrity was accompanied by a concurrent rise of serum bacterial endotoxin level (Fig. 3c) and increased levels of diamine oxidase (DAO) and D-lactic acid, two recognized indicators of intestinal epithelium damage (Fig. 3d, e). In particular, the elevated DAO, also known as histaminase, likely reflects both AGEs-induced enterocyte injury and a compensatory response to heightened histamine levels during allergen sensitization. Upon induction of experimental FA, a markedly decrease in the expression levels of tight-junction (TJ)-related proteins was observed in the intestine of mice fed HAGE relative to the SD control (Fig. 3f and Supplementary Fig. 7a). Similar reduction in TJ-protein expressions was also witnessed in the epicutaneously sensitized model (Supplementary Fig. 7a). This compromised intestinal barrier function may lead to the translocation of noxious compounds, such as microbial metabolites (e.g., lipopolysaccharide (LPS)) and AGEs from lumen into the circulation, subsequently triggering innate danger signaling to prime host immune responses. In light of this, we next assessed the possible activation of relevant receptors (i.e., RAGE and Toll-like receptors (TLRs)) in mouse colon by immunofluorescence staining. An elevated co-expression of RAGE and TLR4 but not TLR2 was observed, suggesting simultaneous activation of both RAGE and TLR4-mediated signaling transduction in the intestine under a high-AGE diet (Fig. 3g and Supplementary Fig. 7b).

Diet-induced dysbiosis of the gut microbiota plays a vital role in inciting aberrant activation of the intestinal mucosal immune system²⁴. We next explored the impact of dAGEs on phylogenetic diversity and relative abundance of the gut microbiota in association with the



compromised gut barrier integrity. Mice fed HAGE showed an increase in the Chao1 index, indicating enhanced species richness, while the total OTUs number and Shannon index remained unchanged, reflecting a selective impact on gut microbiota diversity (Fig. 3i). Principal coordinates analysis revealed clear separations between the HAGE and SD-fed groups at the end of both regimen intervention and allergen sensitization phases (Fig. 3h). Significantly enriched genera in the high-

AGE group include those recognized pathogenic and pro-inflammatory taxa that were able to produce LPS, such as *Alistipes*, *Desulfovibrio*, and *Helicobacter*. In contrast, bacteria involved in the production of short-chain fatty-acids (SCFAs) such as *Bifidobacterium* and *Lachnospirillum* were depleted in the HAGE group (Fig. 3j and Supplementary Fig. 8a–c). Through correlation analysis, the relative abundance of these LPS-producing and SCFAs-producing genera were

Fig. 2 | Long-term intake of dAGEs promoted susceptibility to experimental food allergy. BALB/c mice were fed either a control standard diet (SD) or a heat-treated high-AGE diet (HAGE) for 12 weeks before induction of experimental food allergy via *i.g.* gavage of model allergen OVA. **a** Schematic illustration of the study design[#]. **b** Contents of AGEs in the serum and feces of mice upon 12 weeks of regimen ($n = 5$). **c** Clinical allergy score of mice upon last challenge ($n = 7-8$). **d** Serum total IgE level ($n = 7-8$). **e** Serum OVA-specific antibody level (IgE, IgG1 and IgG2a; $n = 7-8$). **f** Representative images of H&E and Toluidine Blue-stained intestinal sections; scale bar: 50 μm . **g** Mast cell counts per jejunum/colon section ($n = 5$). **h** Mass cytometry t-SNE analysis of MLN lymphocytes (equal sampling across groups, total over 225,000 events). **i** Average frequencies of specific immune cells in MLN lymphocytes ($n = 3-4$). **j** Spearman correlations between the

frequency of immune cell subsets and levels of differentially expressed cytokines in MLN cells ($n = 3-4$). The R values were colorimetrically represented by scale at right. Bar graphs show mean \pm SEM (**b, e, i**) and boxplots represent median with 25th/75th percentiles (box) and 1.5 \times IQR (whiskers) (**c, d, g**). **b** Pair-wise comparison was conducted by Mann-Whitney tests (two-tailed); **c-i** Comparisons were performed using one-way ANOVA or Kruskal-Wallis test, followed by appropriate post hoc tests for pairwise comparisons. * $p < 0.05$, ** $p < 0.01$, *** $p < 0.001$. FDR-corrected q values were presented in correlation analysis. dAGEs dietary advanced glycation end-products, H&E hematoxylin and eosin, *i.g.* intragastric, MLN mesenteric lymph nodes, OVA ovalbumin, tSNE t -distributed stochastic neighbor embedding.

[#]Created in BioRender. Zhang (2025) <https://BioRender.com/pf8iqnb>. Source data are provided as a Source Data file.

significantly correlated with the above epithelium barrier indicators and activation of the innate immune signaling (Fig. 3k and Supplementary Fig. 8d). The epicutaneously sensitized model showed a similar pattern of dysbiotic microbiota linked to the compromised intestinal TJ-protein expression (Supplementary Fig. 9). Taken together, these results provided compelling evidence that prolonged intake of dAGEs promoted intestinal barrier dysfunction and microbiota dysbiosis that facilitated the passage of allergens and bacterial products to perpetuate intestinal allergic inflammation.

dAGEs act as adjuvant stimuli to promote bystander sensitization to food allergen

Long-term exposure of a high-AGE diet promoted immune responses to unrelated allergens in adjuvant-dependent models. We next questioned that whether dAGEs could act as adjuvant stimuli to prime type-2 immune responses to establish allergic sensitization. Using BSA-AGE as a representative form of dAGEs (Supplementary Fig. 10a), we established an FA model to examine the adjuvant activity of BSA-AGE in inducing bystander sensitization to a model allergen OVA. Mice were exposed to BSA-AGE alone or in the presence of OVA via intragastric (*i.g.*) gavage four times a week for 4 weeks (Fig. 4a). Following oral challenge, mice exposed to OVA alone did not manifest signs of FA. In comparison, mice sensitized to OVA in the presence of BSA-AGE developed typical food-allergic symptoms along with a prominent drop in the body temperature indicative of anaphylaxis (Fig. 4b, c). Concurrent increases in antigen-specific antibodies and T-cell responses were also witnessed (Fig. 4d-f). To further confirm that the Th2-skewed immune response was OVA-specific, we performed tetramer analysis using an IAb tetramer specific for the OVA₃₂₃₋₃₃₉ epitope to simulate splenocytes from sensitized mice. The results revealed that compared to OVA control, the AGE + OVA group displayed a significantly higher frequency of CD4⁺ tetramer-positive cells, which provides compelling evidence that AGEs exposure amplifies OVA-specific Th2 responses (Supplementary Fig. 10b). Furthermore, similar to the adjuvant-dependent models, mice exposed to BSA-AGE showed intestinal barrier dysfunction and localized inflammation, as evidenced by the increased intestinal permeability, reduced gene expression of TJ-proteins and up-regulated expression of pro-inflammatory molecules (including RAGE, TLR4 and danger signal molecules) in the intestine (Fig. 4g, h and Supplementary Fig. 10c, d). However, this adjuvant effect of BSA-AGE toward unrelated allergens seems to be restricted to oral routine, as sensitization via intraperitoneal injection (*i.p.*) did not induce antigen-specific responses and Th2-skewing effects as observed in the *i.g.* model (Supplementary Fig. 11). This manifests that the adjuvant activity of BSA-AGE requires GALT-associated stimuli at the oral-mucosal inductive sites.

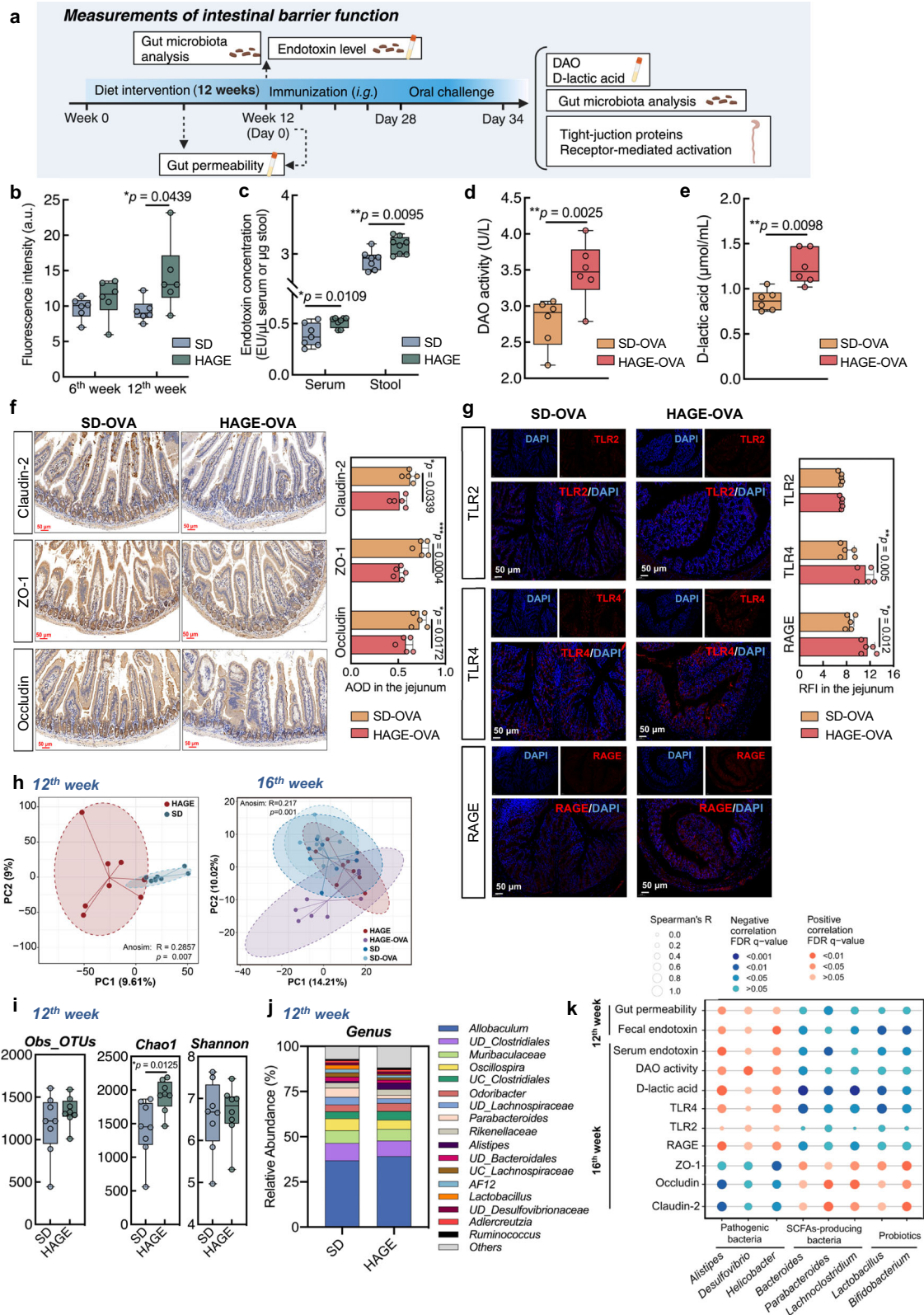
The sensitization priming effect of adjuvant stimuli required altering of the dendritic cells (DCs) phenotype from a phagocytic stage toward a Th2-stimulatory function³¹. We next applied an *ex vivo* bone marrow-derived DCs (BMDCs) model to access the effect of BSA-AGE on the maturation of DCs by flow cytometry (Supplementary Fig. 12a).

In line with previous results in human monocytes³², stimulation with BSA-AGE induced overexpression of key costimulatory molecules in mice BMDCs, particularly class II major histocompatibility complex (MHC-II), an antigen-presenting molecule that is essential for adaptive immunity (Fig. 4i, j). Notably, AGE stimulation significantly upregulated the surface expression of OX40 ligand (OX40L), a Th2-polarizing ligand critical for allergic sensitization (Supplementary Fig. 12b). Furthermore, AGE-induced BMDCs exhibited an accelerated uptake of the OVA allergen, a process that likely enhances antigen presentation and promotes allergic sensitization (Supplementary Fig. 12c). Co-expression of the costimulatory and antigen-presenting molecules on DCs enables their interaction and initiation of down-stream T-cell proliferation, known as a key sentinel in driving the immunostimulatory property of adjuvants like cholera toxin (CT) to establish allergic sensitization^{31,33}. Collectively, these results demonstrate that dAGEs can act as adjuvants to promote innate and adaptive immune responses that potentiate sensitization to bystander allergens in an oral-mucosal dependent way.

Crosstalk between RAGE and TLR4 signaling in dAGEs-induced allergic inflammation

In the above experimental FA models, we observed up-regulation of RAGE and TLR4 signals in the intestine of sensitized mouse when exposed to dAGEs. To understand the role of RAGE/TLR4-signaling in food sensitization manipulated by dAGEs, we performed the adjuvant-free FA model in wild type (WT), RAGE-knockout (RAGE^{-/-}), and TLR4-knockout (TLR4^{-/-}) mice as per the study design (Fig. 5a). The magnitude of food allergic inflammation in response to OVA in the presence of BSA-AGE was significantly reduced in the absence of RAGE or TLR4, as evidenced by the reduced allergy score (Fig. 5b), maintained body temperature upon challenge (Fig. 5c), and decreases in OVA-specific IgE levels (Fig. 5d). Interestingly, while RAGE^{-/-} mice were protected from AGEs-induced allergic symptoms, they showed higher baseline IgE levels compared to WT and TLR4^{-/-} mice. This may result from compensatory mechanisms, such as enhanced TLR4 signaling, which sustain low-level IgE production but fail to drive OVA-specific IgE enhancement or full allergic inflammation. Moreover, neither RAGE^{-/-} or TLR4^{-/-} mice were protected against increases in specific IgG1 production, whereas a reduction in specific IgG2 levels was exclusively observed in RAGE^{-/-} mice, not in TLR4^{-/-} mice (Fig. 5e, f). The differentiation of T cells toward a Th2-biased phenotype was also suppressed in the absence of RAGE or TLR4 (Fig. 5g-i).

To further confirm the crosstalk between RAGE and TLR4 signaling in dAGEs-mediated allergic inflammation, we tested the expression of receptor-mediated signaling and markers related to epithelial barrier function, type-2 immunity and localized inflammation in the intestine of KO mice. In TLR4^{-/-} mice, activation of RAGE was not observed in the AGE + OVA group, while in RAGE^{-/-} mice, up-regulation of TLR4 and its adapter molecule MyD88 can be detected (Fig. 5k). As a consequence, TLR4^{-/-} mice were protected from disruptions in gut barrier integrity and Th2-biased pro-inflammatory responses in the



intestine, whereas significant increases in IL-33 (a danger signal released from damaged epithelium) and a trend toward increased GATA3 (the key transcription factor for Th2 response) expression were still observed in RAGE^{-/-} mice (Supplementary Fig. 13). This suggests that in addition to the stimulatory effect of dAGEs, there exist bystander mechanisms leading to the activation of TLR4-signaling in the absence of RAGE under a high-AGE diet (e.g., bacterial metabolites

from microbiota dysbiosis) (Fig. 5j). However, this effect appears to be insufficient to elicit allergic responses without RAGE signaling. Overall, these results suggest that RAGE and TLR4 signaling pathways likely act in a complex cross-talk manner to mediate AGEs-induced allergic inflammation: TLR4 drives early barrier disruption and localized inflammation, while RAGE is essential for later-stage immune cell activation and allergen-specific responses.

Fig. 3 | Chronic exposure to dAGEs induced intestinal barrier dysfunction and dysbiosis of the gut microflora. a–g To evaluate the effect of dAGEs on intestinal barrier function, a series of experiments were meticulously designed across the dietary intervention and allergen sensitization phases: **a** Schematic illustration of the experimental design⁶. **b** Gut permeability assessed by an FITC-dextran assay ($n = 6$). **c** Endotoxin level in serum and feces of mice ($n = 7–8$). **d** Serum DAO activity ($n = 6$). **e** Serum *D*-lactic acid concentration ($n = 6$). **f** Representative images of immunohistochemistry staining for Claudin-2, ZO-1, and Occludin proteins in the jejunum tissue ($n = 5$); scale bar: 50 μm . **g** Representative images of immunofluorescence staining for RAGE, TLR2, and TLR4 receptors in the colon tissue ($n = 5$); scale bar: 50 μm . **h–k** To assess the impact of dAGEs on gut microbiota composition, feces of mice receiving different regimens were analyzed for 16S rRNA sequencing: **h** PCoA analysis based on Bray–Curtis distance (Anosim test; $n = 8$). **i** Total OTUs number and α -diversity indexes ($n = 8$). **j** Bacterial relative

abundance at the genus level ($n = 8$). UC unclassified, UD unidentified. **k** Spearman correlations between the relative abundance of pathogenic and probiotic genera and indicators associated with epithelium barrier function and innate signaling activation ($n = 5–8$). The R values were depicted by the circle size and color as scaled at the top. Bar graphs show mean \pm SEM (**f, g**) and boxplots represent median with 25th/75th percentiles (box) and $1.5 \times$ IQR (whiskers) (**b–e, i**). Pair-wise comparison was conducted by Student's t tests or Mann–Whitney tests (two-tailed). * $p < 0.05$, ** $p < 0.01$, *** $p < 0.001$; FDR-corrected q values were presented in correlation analysis. AOD average optical density, DAO diamine oxidase, dAGEs dietary advanced glycation end-products, FDR false discovery rate, OTUs operational taxonomic units, PCoA principal coordinate analysis, RFI relative fluorescence intensity, SCFAs short-chain fatty acids. ⁶Created in BioRender. Zhang (2025) <https://BioRender.com/pf8Iqnb>. Source data are provided as a Source Data file.

Modulation of peripheral immune signature by dAGEs involving RAGE and TLR4 signaling: validation results

Once AGEs traverse the barrier and enter the circulatory system, they may elicit inflammation and dysfunction in circulating immune cells. An aberrant functioning of the peripheral immune system underlies the pathogenesis of FA, contributing to the progression of allergies at distant mucosal sites³⁴. Finally, to validate our prior results, we examined the effect of AGEs on peripheral immune signature and cytokine response in PBMCs from healthy individuals (Fig. 6a). We also exposed PBMCs to bacterial metabolites from HAGE-fed mice to see if AGE-mediated gut dysbiosis would affect the immune cells. Exposure to BSA-AGE induced a significant increase in the proportion of Th2 cells, when compared to the cells treated with PBS alone (Fig. 6b, c). In addition, AGE-treatment led to a higher expression of RAGE in both Th1 and Th2 subsets as compared to the control groups. A significant increase in the frequency of TLR4⁺ cells was also observed in Th2 cells in the AGE group than that seen in the controls. Meanwhile, exposure of PBMCs to FM-HAGE, a fecal supernatant containing bacterial products from HAGE-fed mice (Fig. 2a), elicited a significant increase in the proportion of Th2 cells (Fig. 6b, c). Additionally, TLR4 expression in both Th1 and Th2 cells were tended to be higher in the FM-HAGE group compared to the FM-SD control. This Th2-polarizing and pro-inflammatory effect of AGE and associated metabolites was further evidenced by cytokine production in PBMCs. While AGE exposure alone showed a modest, non-significant trend toward increased secretion of Th2 (IL-4, IL-5) and pro-inflammatory cytokines (TNF), exposure to FM-HAGE significantly enhanced the production of these cytokines (Supplementary Fig. 14). Together, these data validated the capacity of AGEs and their microbiota-derived metabolites to promote Th2 polarization and pro-inflammatory responses, primarily through multifaceted mechanisms involving RAGE and TLR4 signaling pathways.

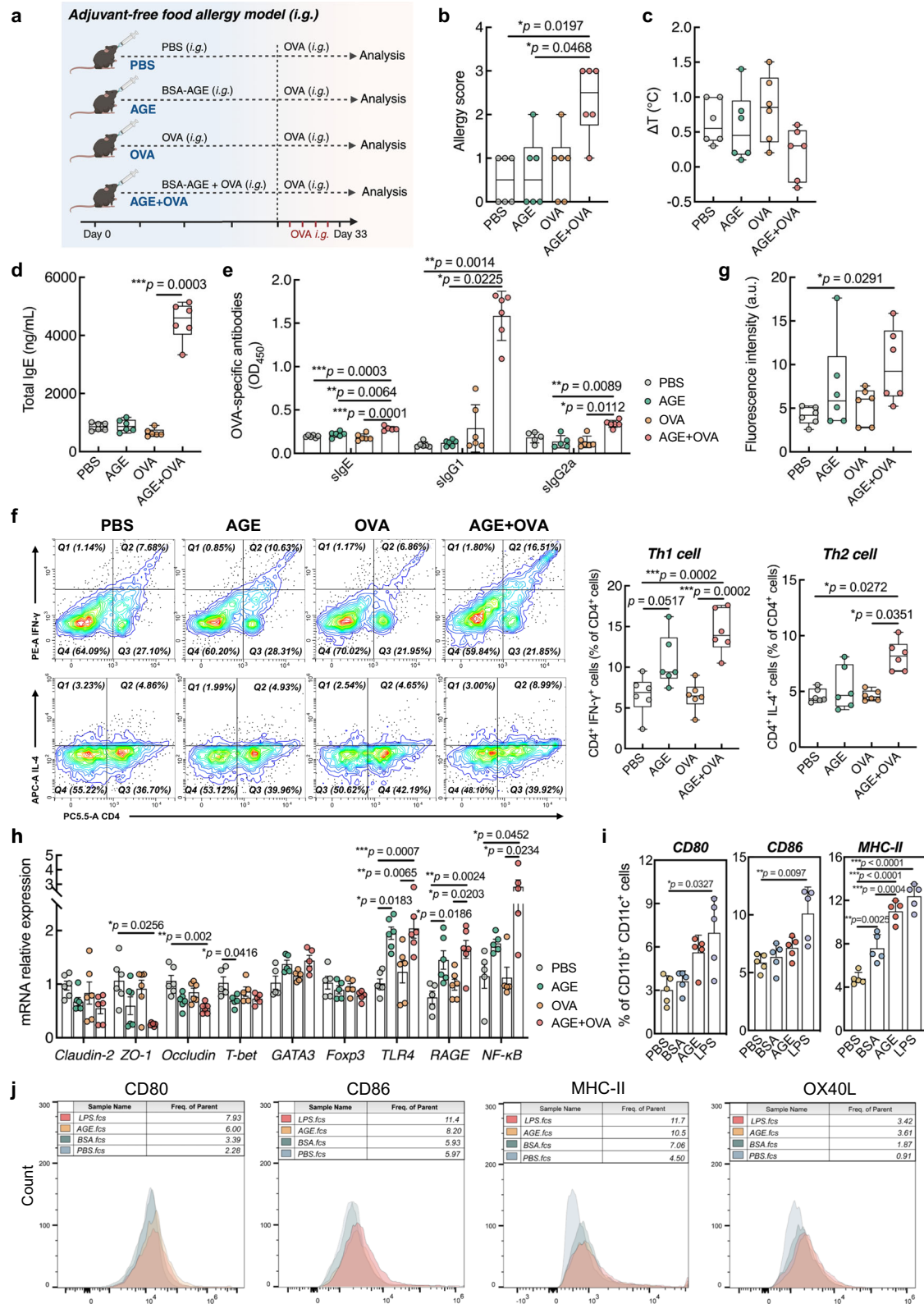
Discussion

The steep increase in the prevalence of FA in the past decades suggests that, other than genetic predisposition, environmental factors linked to modernization are important drivers of this epidemiologic scenario^{2,35}. Changes in dietary habits associated with Western lifestyles have been raised as a key contributor to this surge in allergic conditions. It is apparent that the modern Western diet is overindulged in UPFs that are not only laden with fats and sugars, but are also a prominent source of dAGEs, a group of detrimental compounds ubiquitously generated during thermal processing^{22,28}. Observational studies have suggested a link between the consumption of foods high in AGEs (e.g., fast food) and the risk of developing FA^{26,28}. In this study, we first presented population-based, cross-sectional data supporting that a dietary pattern rich in AGE-containing UPFs is associated with increased prevalence of self-reported allergic diseases, including FA. Further, through multiple experimental models of FA, we demonstrated that chronic exposure to a high-AGE diet exacerbates allergic

inflammation and promotes Th2-skewed immunity toward bystander food allergens. Intake of dAGEs disrupted the intestinal barrier integrity and functioned like adjuvants to stimulate Th2-biased immune responses at mucosal sites, ultimately leading to the misinterpretation of dietary allergens to trigger allergic reactions.

By employing multiple experimental models of FA, we revealed distinct immunological outcomes that underscore the pivotal role of AGEs in promoting allergic sensitization. In the orally sensitized model, we observed increased mast cell infiltration and Th2 cell frequency in the intestine mucosa, despite the absence of concurrent rises in allergen-specific antibodies. Notably, the enhanced mast cell expansion and degranulation in the HAGE groups support that prolonged consumption of a high-AGE diet can induce allergic inflammatory responses, even after a few doses of antigen exposure. These findings align with previous studies demonstrating that mast cells play a critical role in the pathogenesis of food allergy by releasing histamine and other pro-inflammatory mediators upon allergen exposure. Similarly, in the epicutaneously sensitized model, we observed a significant elevation in serum total IgE levels in HAGE-fed mice, along with a higher frequency of Th2 cells and effector cells in the lamina propria. Furthermore, the adjuvant-free model provided compelling evidence that dAGEs can directly promote Th2-mediated allergic responses without the need for additional adjuvants. Mice exposed to BSA-AGE in the presence of OVA developed typical food-allergic symptoms, including an increased allergy score and elevated levels of OVA-specific antibodies and Th2 immune responses. These findings suggest that dAGEs can act as standalone adjuvants to prime the immune system for allergic sensitization. Overall, the consistent observation of Th2-skewed immune responses, elevated IgE production, and mast cell activation across different models highlights the potential of AGEs as a key factor driving the increasing prevalence of FA in Westernized diets.

There is a consensus that defects in intestinal barrier function predispose to allergic and autoimmune diseases³⁰. Loss of the gut epithelial integrity allows for an excessive influx of allergen-derived peptides and bacterial metabolites that constantly prime both adaptive and innate immune cells to elicit an aberrant Th2 immunity. In this study, we observed that prolonged intake of a high-AGE diet induced increases in gut permeability, in concurrency with dysbiosis of the gut microbiota and translocation of bacterial products in vivo. These alterations preceded the sensitization of Th2-polarized immune responses toward a concomitant food allergen. It is postulated that dAGEs in heat-processed foods can act as epithelial barrier-damaging agents that perpetuate chronic inflammation in epithelial cells, ultimately driving intestinal barrier dysfunction. In our prior in vitro study in Caco-2 cells, exposure to AGEs augmented pro-inflammatory cytokine production and perturbed the expression of TJ-proteins in a dose-dependent manner³⁶. Qu et al. reported that, long-term intake of a heat-treated diet led to alterations in colonocyte structure and reduced the expression of TJ-proteins in the colon of a rat model¹⁹. Moreover, diet-induced dysbiosis of the gut microbiota has been



implicated in the pathogenesis of intestinal barrier damage and food sensitization²⁴. In fact, due to the presence of cross-linking structures and unnatural amino acid modifications, dAGEs are less available for absorption in the upper gut because of their reduced susceptibility to digestive enzymes^{37–39}. As a result, a considerable amount of digestion-resistant dAGEs reach the colon and undergo anaerobic fermentation, reciprocally altering the composition and function of the gut microflora¹². Despite inconclusive, previous studies have observed that

consumption of heat-processed foods containing AGEs can modulate the composition of gut microbiota in both rodent models and humans^{22,40}. In healthy adolescents, intake of high-AGE diets favored putatively harmful bacteria in the intestinal microbiota, as evidenced by the decreased levels of *Lactobacillus* and *Bifidobacterium* genera⁴⁰. Probiotic bacteria, such as *Lactobacillus*, is capable of producing the enzyme glyoxalase to degrade dAGEs, and its abundance is closely associated with the development of oral tolerance to antigens^{41–43}.

Fig. 4 | dAGEs act as mucosal adjuvants to stimulate Th2-mediated allergic responses to a concomitant food allergen. a–h To explore the Th2-adjuvant activity of dAGEs, C57BL/6J mice were exposed to BSA-AGE alone or in the presence of model allergen OVA via *i.g.* gavage to establish an adjuvant-free model of food allergy: **a** Schematic illustration of the study design[#]. **b** Clinical allergy score of mice upon last challenge ($n = 6$). **c** Rectal temperature change after last challenge ($n = 6$). **d** Serum total IgE level ($n = 6$). **e** Serum OVA-specific antibody level (IgE, IgG1 and IgG2a; $n = 5–6$). **f** Representative cell sorting plots and quantification of Th1 and Th2 cells in MLN lymphocytes by flow cytometry ($n = 6$). **g** Gut permeability assessed by an FITC-dextran assay ($n = 6$). **h** Relative expression levels of genes related to intestinal barrier integrity, type 2 immunity, and pro-inflammatory responses in the intestine ($n = 5–6$). **i, j** Mouse BMDCs were *ex vivo* treated with BSA-AGE to assess its

effect on DCs phenotype ($n = 5$). PBS/BSA- and LPS-treated cells were the negative and positive controls, respectively. Flow cytometry of CD80⁺, CD86⁺, MHC-II⁺, and OX40L⁺ cells in CD11b⁺ CD11c⁺ cells were analyzed. Bar graphs show mean \pm SEM (**e, h, i**) and boxplots represent median with 25th/75th percentiles (box) and $1.5 \times$ IQR (whiskers) (**b–d, f, g**). Comparisons were performed using one-way ANOVA or Kruskal–Wallis test, followed by appropriate post-hoc tests for pairwise comparisons. * $p < 0.05$, ** $p < 0.01$, *** $p < 0.001$. BMDCs bone marrow-derived dendritic cells, BSA-AGE methylglyoxal-glycated bovine serum albumin, dAGEs dietary advanced glycation end-products, *i.g.* intragastric, LPS lipopolysaccharide, MHC-II class II major histocompatibility complex, MLN mesenteric lymph nodes, OVA ovalbumin, OX40L OX40 ligand. [#]Created in BioRender. Zhang (2025) <https://BioRender.com/pf8S1qnb>. Source data are provided as a Source Data file.

Similar to previous findings, we demonstrated that chronic intake of a high-AGE diet shifted the colonic microbiota of a mouse model toward a more detrimental profile, as characterized by the richness of pathogenic bacterial species and depletion of probiotic and SCFA-producing genera. This distinct microbial feature was intimately linked to the observed disturbances in epithelium barrier integrity and pro-inflammatory signaling in the intestine. Prolonged intake of dAGEs facilitated the colonization of opportunistic pathogens and triggered inflammation within epithelial cells, thereby instigating a vicious circle of leaky barriers, microflora dysbiosis and localized inflammation that increases the susceptibility of developing allergies.

Immune-modulatory agents possessing a Th2-skewing ability may act as adjuvants to promote allergic sensitization to concomitant allergens⁴⁴. This phenomenon has been reported in the context of environmental pollutants, such as diesel exhaust particles and house dusts, and emulsifiers found in processed foods^{45–47}. Here, we demonstrated that dAGEs could act as mucosal adjuvants to stimulate IgE-mediated allergic response and Th2 immunogenicity to a model food allergen. AGEs-induced intestinal barrier dysfunction and inflammation were also evident, as marked by the increased gut permeability, reduced expression of TJ-proteins, localized synthesis of pro-inflammatory cytokines, and activation of the innate signaling pathways (e.g., RAGE). Noteworthy, the adjuvant capacity of AGEs was not observed when given parenterally, indicating that its adjuvant activity is limited to its inductive capacity at the intestinal mucosal sites. AGEs can mimic alarmins to bind with RAGE expressed on epithelial cells, leading to epithelial injury and triggering the release of danger signal molecules including IL-25, IL-33, and TSLP^{25,28}. These epithelial-derived cytokines can further engage DCs and other immune cells to promote the differentiation and activation of Th2 cells²³. In this scenario, Th2 adjuvants are recognized for their capability to modulate the function of DCs from a tolerogenic state to a Th2-polarizing phenotype⁴⁴. Previous studies stimulating DCs with glycated food allergens containing AGEs have demonstrated an enhanced uptake of antigens and excessive production of Th2-promoting cytokines^{48,49}. Our study demonstrated that stimulation with AGEs up-regulated the expression of costimulatory and antigen-presenting molecules on DCs. Up-regulation of costimulatory molecules on DCs elicited by exogenous stimuli constitutes a prerequisite for the enhancement of allergen-specific Th2 immune response⁵⁰. These results, together with previous findings, indicate that AGEs could act as adjuvants with the capacity to activate DCs toward a pro-allergenic phenotype that specifically signals native T cells to Th2 differentiation.

Previous studies have reported that RAGE is highly expressed on multiple immune cells, including DCs, T lymphocytes, macrophages, and B cells, as well as mast cells and basophils^{28,51}. Besides, it has been demonstrated that T-cell priming and proliferation is dependent on RAGE ligation and DCs require RAGE signaling for migration to the draining lymph nodes after antigen exposure^{52,53}. In addition, the RAGE receptor shares common ligands with TLR4, and both have a similar mechanism of action to exert a synergistic effect on activation of the

downstream signaling pathways^{51,54,55}. There exist evidence suggesting that AGEs can stimulate both RAGE and TLR4 signaling in mammalian cells to elicit pro-inflammatory reactions^{56,57}. It was also reported that RAGE-deficient mice showed reduced allergic response and airway inflammation toward inhaled allergens in mouse models of asthma^{51,58}. Additionally, TLR4 is also recognized as the receptor for bacterial endotoxins (e.g., LPS) and ligation of TLR4 operates down-stream signal transduction in an adapter-dependent way⁵⁹. In this study, we found that mice lacking either RAGE or TLR4 were protected from AGEs-mediated allergic responses. dAGEs can act as ligands for both RAGE and TLR4 expressed on epithelial and immune cells, thereby initiating down-stream signaling cascades to promote localized inflammation and type-2 immunity. This is further validated in human PBMCs that AGEs-exposure promoted Th2 differentiation and pro-inflammatory responses involving activation of the RAGE and TLR4 signaling axes. Interestingly, in RAGE-deficient mice, we observed up-regulation of TLR4 and its adapter molecule MyD88, along with elevated IL-33 levels and a trending higher GATA3 expression in the intestine. However, activation of TLR4 alone is insufficient to drive the full Th2 immune response required for allergic sensitization. These findings suggest that TLR4 and RAGE signaling may contribute to distinct stages of dAGEs-induced allergic inflammation: TLR4 drives early barrier disruption and localized inflammation, while RAGE is essential for later-stage immune cell activation and allergen-specific responses. In this context, it should also be mentioned that bacterial metabolites from dAGEs-induced gut dysbiosis may also contributed to augmented inflammation and Th2 immunity by activating the TLR4 pathway post-circulatory entry. Therefore, it can be summarized that, dAGEs disrupt the integrity of the intestinal barrier, leading to an increased permeability that facilitated the entry of luminal antigens, digestion-resistant AGEs and pathogenic bacteria into the lamina propria and peripheral circulation. This exposure triggers a constant priming of mucosa inflammation and type 2 immune responses by initiating a series of transduction cascades, ultimately leading to the misinterpretation of food allergens as threats to elicit allergic reactions (Fig. 7).

Despite making a significant contribution to the understanding of dAGEs in facilitating FA, the current study is limited in one that heat treatment of the chow diet yielded a complex mixture of diverse AGEs, rather than a homogenous compound. Besides, the presence of other Maillard reaction products, distinct from AGEs, may also contribute to the observed Th2-mediated allergic responses. Future studies should focus on the examination of individual AGEs to delineate their specific effects across various AGEs moieties on the mucosal immunity. Nonetheless, it should be noted that heat-processed foods consumed in real-life scenarios contain a myriad of AGEs, and our study aims to authentically represent the genuine impact of these compounds on the human health. Another limitation is that we adopted conventional KO mouse instead of double KO mouse or tissue-/cell-specific KO models. Subsequent research employing targeted genetic manipulation would help to elucidate the precise role of RAGE-TLR4 crosstalk

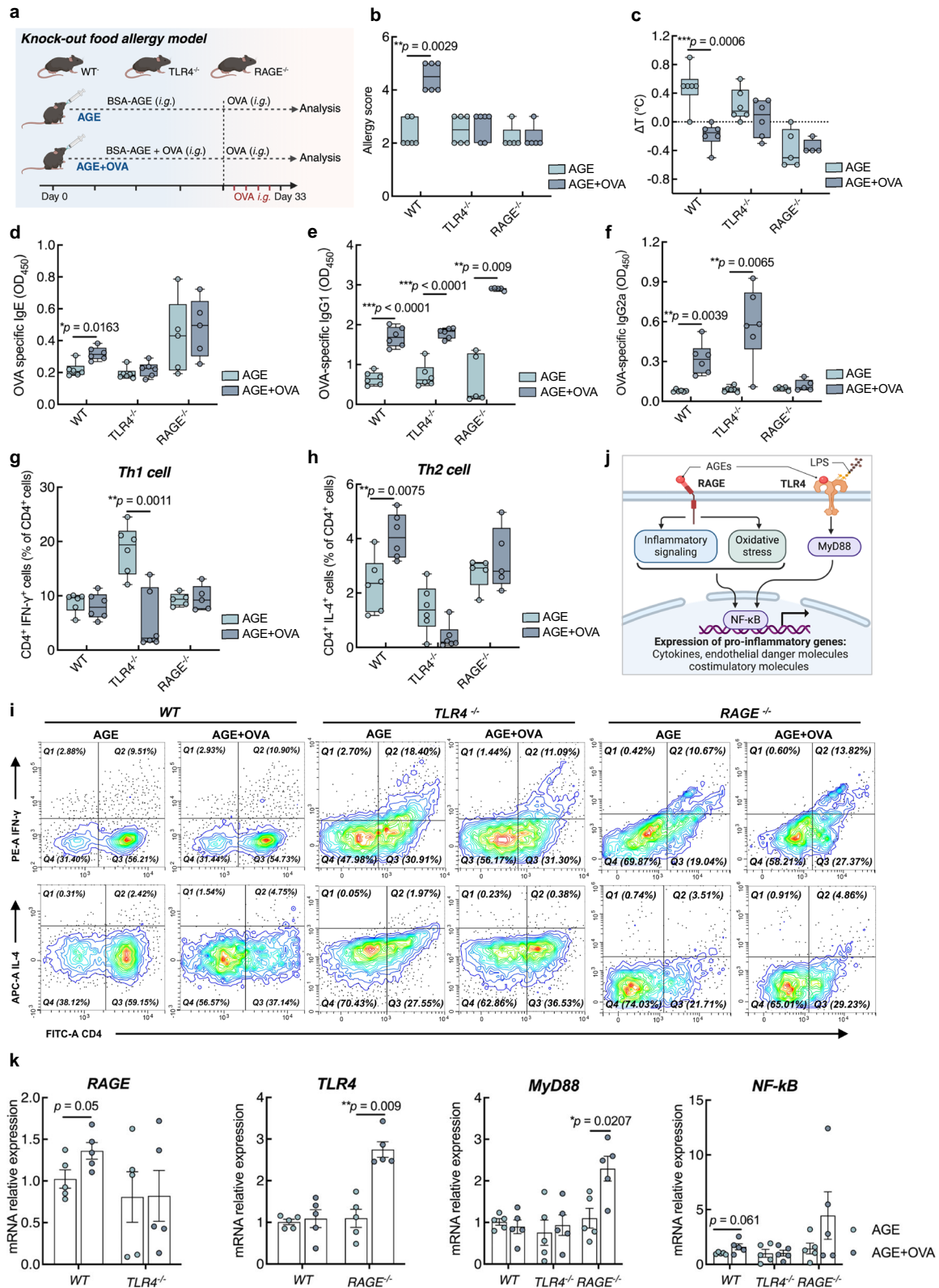


Fig. 5 | The role of RAGE-TLR4 crosstalk in dAGEs-induced allergic inflammation. To elucidate the role of RAGE/TLR4-signaling in food allergic responses manipulated by dAGEs, the adjuvant-free model of food allergy was re-performed in wild type (WT), RAGE-knockout (RAGE^{-/-}), and TLR4-knockout (TLR4^{-/-}) mice. **a** Schematic illustration of the study design[#]. **b** Clinical allergy score of mice upon last challenge. **c** Rectal temperature change after last challenge. **d** Serum OVA-specific IgE level. **e** Serum OVA-specific IgG1 level. **f** Serum OVA-specific IgG2a level. **g–i** Representative cell sorting plots and quantification of Th1 and Th2 cells in MLN lymphocytes by flow cytometry. **j** Interplay between RAGE and TLR4 signaling

pathways[#]. **k** Relative expression levels of genes related to receptor-mediated signaling in the intestine. Bar graphs show mean \pm SEM (**k**) and boxplots represent median with 25th/75th percentiles (box) and 1.5 \times IQR (whiskers) (**b–h**). $n = 5–6$. Pair-wise comparison was conducted by Student's *t* tests or Mann–Whitney tests (two-tailed). * $p < 0.05$, ** $p < 0.01$, *** $p < 0.001$. BSA-AGE methylglyoxal-glycated bovine serum albumin, dAGEs dietary advanced glycation end-products, OVA ovalbumin. [#]Created in BioRender. Zhang (2025) <https://BioRender.com/pf8iqnqb>. Source data are provided as a Source Data file.

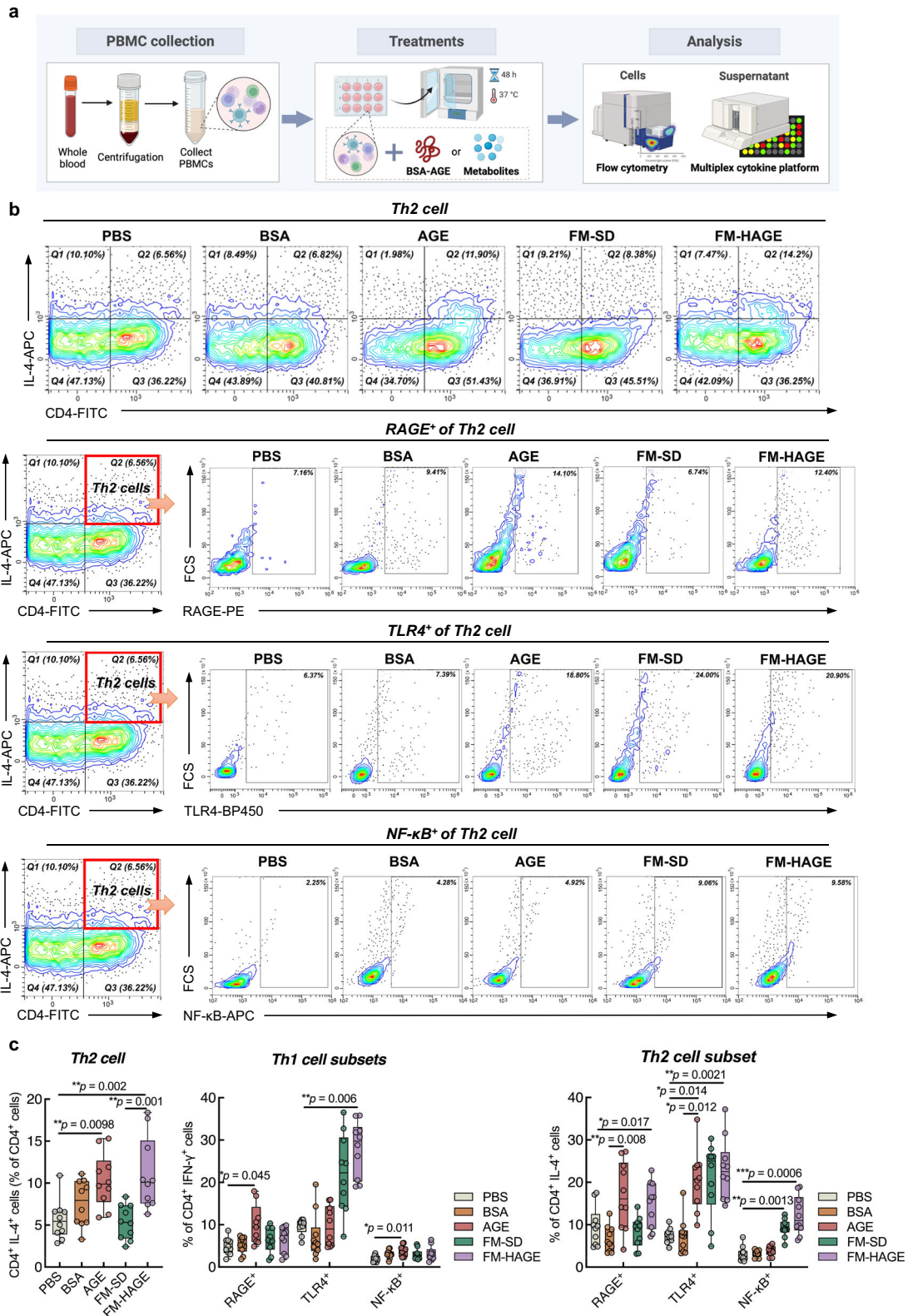


Fig. 6 | Validation of dAGEs-induced Th2-stimulating and pro-inflammatory response in human PBMCs. To validate the Th2-stimulating and pro-inflammatory effect of dAGEs, PBMCs from healthy individuals were stimulated with BSA-AGE (AGE) or a fecal supernatant (FM-HAGE) from HAGE-fed mice of the orally sensitized model, before using flow cytometry for Th-cell subset analysis. Cells treated with PBS, BSA, and a fecal extract (FM-SD) from SD-fed mice served as negative controls. **a** Schematic illustration of the study design[#]. **b, c** Representative cell sorting plots and quantification of Th1, Th2 cells and their subsets in treated PBMCs

by flow cytometry. Results represent median with 25th/75th percentiles (box) and 1.5 × IQR (whiskers). *n* = 9–10. Comparisons were performed using one-way ANOVA or Kruskal–Wallis test, followed by appropriate post-hoc tests for pairwise comparisons. **p* < 0.05, ***p* < 0.01, ****p* < 0.001. BSA-AGE methylglyoxal-glycated bovine serum albumin, dAGEs dietary advanced glycation end-products. [#]Created in BioRender. Zhang (2025) <https://BioRender.com/pf8iqnb>. Source data are provided as a Source Data file.

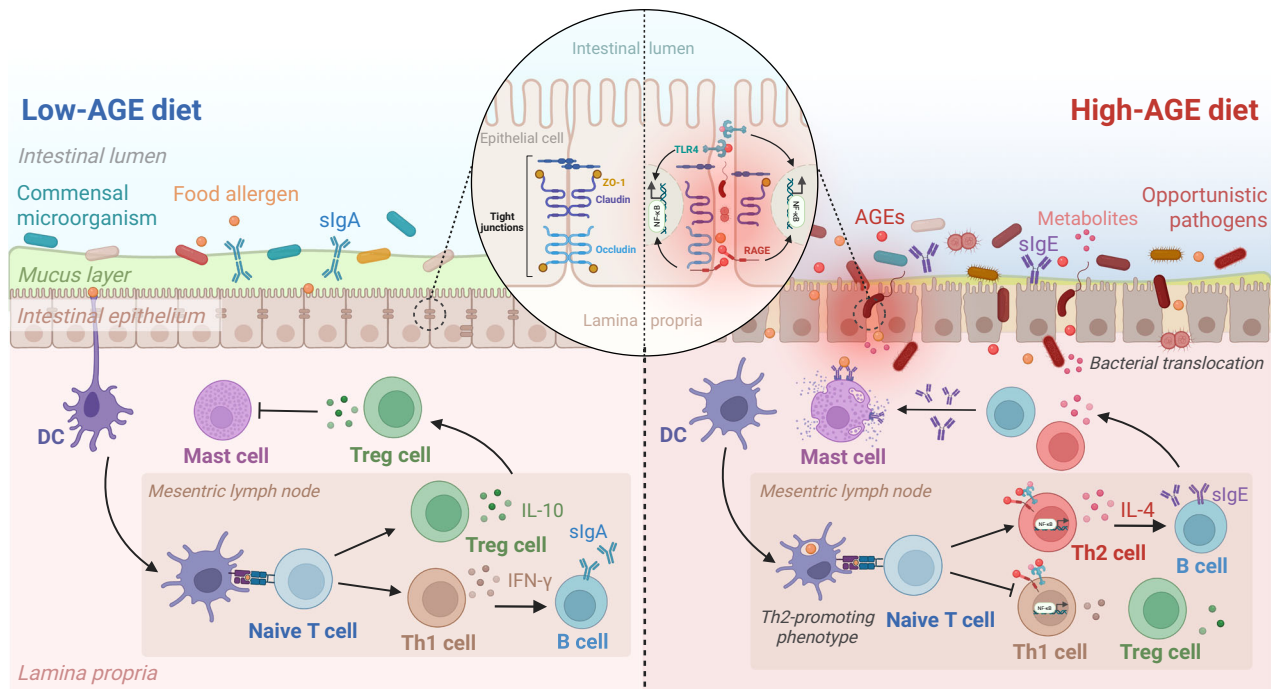


Fig. 7 | Schematic diagram of the mechanism underlying dAGEs-promoted susceptibility to food allergy. Exposure to dAGEs disrupts the intestinal barrier integrity, resulting in an increased permeability that allows for the entry of luminal antigens, digestion-resistant AGEs and pathogenic bacteria into the lamina propria and peripheral circulation. This exposure triggers a constant priming of mucosa

inflammation and type 2 immune responses by initiating a series of transduction cascades, ultimately leading to the misinterpretation of food allergens as threats to elicit allergic reactions. Created in BioRender. Zhang (2025) <https://BioRender.com/pf8iqnb>.

on specific cell types in manipulation of the intricate interplay between dAGEs and allergic sensitization.

In conclusion, this study provides complementary epidemiologic and experimental data elucidating the pathogenic role of dAGEs from processed foods in facilitating the development of FA. Consumption of dAGEs induced an alert gut epithelium and intestinal barrier dysfunction that facilitated down-stream type 2 immunity through innate signaling cascades, ultimately leading to the misinterpretation of food allergens as threats. These results contributed to our understanding of the risk factors for FA in the modern Western diet and offered a preventive strategy for restricting dAGEs consumption to limit allergic susceptibility in predisposed populations. Given the involvement of AGEs in multiple diseases to represent one of the most modifiable factors, targeting AGEs through dietary or therapeutic interventions may offer a promising strategy for improving public health. Our study also highlighted the necessity of future inquiries into other putatively noxious ingredients in UPFs, such as synthetic colorants, emulsifiers, and preservatives, to fully clarify the contributory role of UPFs in escalating allergic conditions and to ascertain their adverse impacts on human health.

Methods

The NHANES database

We used nationally representative data from the NHANES 2007–2010 to evaluate the association between intake of AGEs-containing UPFs and the prevalence of allergic diseases. A total of 13,022 participants were selected after sequentially excluding 7664 participants ≤ 5 and ≥ 60 years old and 1257 participants with missing data (Supplementary Fig. 1). Intake of UPFs was assessed based on the two 24-h dietary recalls of NHANES and reported as the average percentage of total energy consumption from UPFs as previously described^{10,60}. Categorization of UPFs was guided by the definitions of the NOVA food classification system⁷ and screened based on the variables “Main Food Description”, “Additional Food Description”, and “SR Code Description” from the NHANES 24-h

recall datasets. The variables “Combination Food Type” and “Source of Food” were also considered when necessary. Details of the assessment method can be referred to previous reports⁶⁰. Additionally, dietary fiber intake and the Composite Dietary Antioxidant Index (CDAI) were calculated from dietary recalls. The CDAI was derived from six dietary antioxidants: vitamin A, vitamin C, vitamin E, zinc, selenium, and carotenoids. Each antioxidant intake was standardized by subtracting the mean and dividing by the standard deviation, and the standardized values were summed to calculate the CDAI^{61,62}. In parallel, the prevalence of self-reported allergic symptoms was identified by a positive response to the question, “Do you have any food allergies? / Has a doctor ever told you have asthma? / In the past 12 months, have you had wheezing or whistling in your chest”⁶³. Multivariable logistic regression was used to estimate the associations between UPFs intake (Quartile) and allergic disorders, with adjustment covariates including dietary fiber, CDAI, age (6–12, 13–19, 20–39, 40–59), sex (male and female), race/ethnicity (non-Hispanic white, non-Hispanic black, Mexican-America, other Hispanic, and other race), education level (high school as a midpoint), and BMI (categorized into normal weight < 25 , $25 \leq$ overweight < 30 , and $30 \leq$ obesity). *p* for trend was calculated using the median value of each quartile as a continuous variable in each model.

Mice

Female wild-type C57BL/6J or BALB/c mice (4–6 week) were purchased from the Laboratory Animal Research Center of Zhejiang Academy of Medical Sciences (Zhejiang, China). Female RAGE^{-/-} and TLR4^{-/-} mice on a C57BL/6J genetic background were generated at the Shanghai Model Organisms Center, Inc. (Shanghai, China). Mice were housed in specific pathogen-free conditions and provided access to chow and water ad libitum, with temperature kept at $22 \pm 1^\circ\text{C}$ and relative humidity of $55\% \pm 10\%$ under a 12-h light-dark cycle. Prior to experiments, mice were randomized to avoid any incidental pre-diet differences and were acclimatized to the animal facility environment for 1 week before any treatments. All animal experiments were carried out

in strict accordance with the National Guidelines for the Care and Use of Laboratory Animals of China and were approved by the Zhejiang Gongshang University Ethics Review Committee (No. 2022032001). In particular, mice were monitored daily for signs of distress, including weight loss $\geq 20\%$, severe diarrhea, or irreversible morbidity, as predefined humane endpoints per institutional guidelines. No adverse effects attributed to adjuvants exposure were observed during the study.

Unless otherwise specified, mice were fed with a standard D12450H diet. For regimen intervention studies, mice received either a control standard diet (D12450H) or a heat-treated high-AGE diet (D12450H baked at $175\text{ }^{\circ}\text{C}$ for 45 min^{18}) for 12 weeks before induction of experimental FA. Both diets were sourced from Xietong Bioengineering Co., Ltd. (Nanjing, China) and were free of allergens and identical in calories and macronutrients level (Supplementary Table S2).

Experimental models of FA

Orally sensitized FA model. BALB/c mice were fed a control standard diet or a high-AGE diet for 12 weeks, followed by induction of experimental FA. Mice were sensitized by *i.g.* gavage of 5 mg OVA with 10 μg adjuvant of CT (Sigma-Aldrich) in 0.2 mL PBS four times per week for 3 weeks. The control group received an equivalent volume of PBS plus CT via *i.g.* gavage. On days 22–25, all mice were challenged by *i.g.* gavage of 50 mg OVA in 0.2 mL PBS for 4 consecutive days ($n = 7\text{--}8$ mice/group).

Epicutaneously sensitized FA model. C57BL/6J mice were fed a control standard diet or a high-AGE diet for 12 weeks, before induction of experimental FA. Mice were sensitized daily with 2 nmol of MC903 (calcipotriol; Sigma-Aldrich) in 20 μL of 100% ethanol on both ears, followed by applying 100 μg OVA in 10 μL PBS on dried ears on the apical side for 14 consecutive days⁶⁴. The control group received the same volume of ethanol and OVA as above. On days 14 and 17.5, all mice were challenged by *i.g.* gavage of 50 mg OVA in 0.2 mL PBS ($n = 8$ mice/group).

Adjuvant-free FA model. To explore the immune-adjuvant activity of AGEs in FA, BSA-AGE, a well-characterized and physiologically relevant dAGEs, was prepared by glycation of bovine serum albumin (BSA) with methylglyoxal (MGO) at $50\text{ }^{\circ}\text{C}$ for 96 h. The mixture was then dialyzed against distilled water at $4\text{ }^{\circ}\text{C}$ for 48 h to remove excessive MGO and salts. C57BL/6J mice were *i.g.* gavaged with either 0.2 mL PBS, or 0.2 mL PBS containing BSA-AGE (5 mg), OVA (5 mg), or BSA-AGE (5 mg) plus OVA (5 mg) five times per week for 4 weeks. The gavage dose of BSA-AGE is selected base on the estimated daily intake of AGEs by an adult as previously indicated⁶⁵. On days 29–32, all mice were challenged by *i.g.* gavage of 50 mg OVA in 0.2 mL PBS for 4 consecutive days ($n = 6$ mice/group). In separate experiments, mice were also treated with BSA-AGE or BSA-AGE plus OVA via *i.p.* following the same protocol as described above.

Knock-out FA model. To investigate the role of RAGE/TLR4-signaling in dAGEs-mediated allergic inflammation, wild type (WT), RAGE-knockout (RAGE^{-/-}), and TLR4-knockout (TLR4^{-/-}) mice were administered BSA-AGE with or without the allergen OVA, following the experimental design of the adjuvant-free model ($n = 5\text{--}6$ mice/group). On days 29–32, all mice underwent repeated oral OVA challenges as previously described.

Upon the last oral challenge, mice were individually recorded for rectal temperature and assessed for clinical allergy score within 30 min (Supplementary Table S3), as described before⁶⁶. Mice were anesthetized and sacrificed by cervical dislocation. Blood was collected to prepare serum fraction, and the MLN, small and large intestinal tissues were harvested under sterile conditions. Fresh feces were also collected and snap-frozen with liquid nitrogen before storage at $-80\text{ }^{\circ}\text{C}$.

Intestinal permeability

Intestinal permeability was assessed *in vivo* by the previously described FITC-dextran assay²⁹. Mice were fasted for 4 h and orally gavaged with 4-kDa FITC-dextran (60 mg/100 g body weight; assessed at week 6/Fri, week 12/Fri in the oral sensitization model, and day 19 in the adjuvant-free model; Figs. 3a and 4a) (Sigma-Aldrich). Blood was collected 4 h after gavage via eye canthus and serum prepared by centrifuging at $10,000 \times g$ for 10 min at $4\text{ }^{\circ}\text{C}$. The serum was diluted 1:10 in PBS, and measured for fluorescence intensity with excitation at 485 nm and emission at 535 nm using a fluorescence spectrophotometer.

Serum and fecal endotoxin level was determined with the Pierce™ Chromogenic Endotoxin Quantitation kit (Thermo Scientific, #A39552), per the manufacturer's instructions. Serum *D*-lactic acid level was quantified using a *D*-lactic acid Content Assay Kit (Solarbio, Beijing, China, #BC5355) and serum DAO activity was measured with a DAO Activity Assay Kit (Solarbio, #BC1285).

AGEs quantification

Mouse fecal samples were lyophilized and powdered, chow diet samples were isolated for protein using chloroform-methanol (2:1, v/v), and serum samples were directly analyzed. Each portion of feces ($\sim 10\text{ mg}$), chow diet (5–10 mg protein) or serum sample (30 μL) was reduced by 2 mL of sodium borohydride solution (1 M in 0.1 M NaOH) at room temperature for 3 h. The reduced sample was then hydrolyzed with 2 mL of HCl (6 M) under nitrogen at $110\text{ }^{\circ}\text{C}$ for 24 h. Afterward, 1 mL of the hydrolysate was dried under vacuum and reconstituted in 2 mL of distilled water. After filtration through a 0.22- μm membrane, the filtrate was mixed with the internal standard mixture prior to analysis by an isotope dilution UHPLCQqQ-MS/MS-based method as previously established¹⁵. Nine types of AGEs, namely CML, CEL, MG-Hs, glyoxal-derived hydroimidazolone isomers (G-Hs), methylglyoxal lysine dimer (MOLD), glyoxal lysine dimer (GOLD), pentosidine, and argpyrimidine were quantified.

Antibody and cytokine analyses

Total serum IgE concentration was determined with a commercially available ELISA kit (Thermo Fisher Scientific, #88-50460-86), following the manufacturer's protocol. Serum OVA-specific IgE, IgG1, and IgG2a were determined by indirect ELISA as previously described²⁰.

Cytokine profiles in *ex-vivo* activated MLN cells were analyzed. Single-cell suspensions from MLN were cultured in complete media (RPMI 1640 containing 10% fetal bovine serum, 1% sodium pyruvate, and 1% penicillin/streptomycin) and stimulated with phorbol 12-myristate 13-acetate (PMA)/ionomycin for 6 h⁶⁷. Cell-free supernatants were measured for multiplex cytokine levels with a Bio-Plex Mouse Cytokine 23-Plex Panel Kit (Bio-Rad, Hercules, CA, USA, #M60009RDPD) on a Bio-Plex 200 System.

Mass cytometry

In the orally sensitized model, single-cell suspensions of MLN were isolated and stimulated with PMA/ionomycin for 6 h as above. In the epicutaneously sensitized model, single-cell suspensions of lamina propria lymphocytes were prepared from mouse small intestine as previously described⁶⁸. The isolated cells were resuspended in chilled PBS, and subjected to Live/Dead staining with 2 μM cisplatin (Fluidigm) for 2 min before quenching with cell staining buffer (CSB; Fluidigm). For surface staining, the cells were counted, diluted to 1×10^6 cells/mL, and incubated with a surface antibody cocktail (Supplementary Table S4) in a total volume of 50 μL CSB for 30 min at room temperature. Then, the cells were washed, permeabilized with 80% methanol, and stained with an intracellular antibody cocktail under identical conditions. After three washes in CSB, cells were resuspended in 0.125 μM Ir-intercalator in Fix and Perm Buffer (Fluidigm) at $4\text{ }^{\circ}\text{C}$ overnight. Finally, the cells were triple washed with ice-cold PBS and deionized water separately. Prior to CyTOF acquisition, cells were

resuspended in deionized water containing 10% EQ Four Element Beads (Fluidigm) at a concentration of 1×10^6 cells/mL and analyzed on a Helios mass cytometer (Fluidigm; Novogene Bioinformatics Technology Co., Ltd., Beijing, China).

The original FCS data were normalized with CyTOF software version 6.7.1014 (Fluidigm) and .fcs files were collected. All .fcs files were uploaded into Cytobank for data cleaning and population of single living cells (Supplementary Fig. S4). viSNE maps were generated with software tools available at www.cytobank.org using the specified markers to perform clustering. Data were then manually gated by using FlowJo 10.6.1 for investigating the cell subsets of interest.

Flow cytometry

For analysis of Th1 and Th2 cell proportions in MLN lymphocytes, single-cell suspensions of MLN were stimulated with eBioscience™ Cell Stimulation Cocktail containing PMA, ionomycin, brefeldin A, and monensin for 6 h at 37 °C. The stimulated cells were first stained with cell-surface marker of FITC anti-mouse CD4 antibody. After fixation and permeabilization, cells were stained with intracellular markers namely APC anti-mouse IFN- γ and PE anti-mouse IL-4 antibodies. Analysis of labeled cells was performed with a CytoFLEX Flow cytometer (Beckman Coulter, Inc., Brea, CA, USA), and data were analyzed by CytExpert software (Version 2.0, Beckman Coulter, Inc., Brea, CA, USA; Supplementary Fig. S4).

Tetramer analyses of OVA-specific T-cell responses

Mice were sensitized with OVA protein with or without BSA-AGE for 4 weeks as per indicated in the adjuvant-free model. On day 29 and 30, mice were challenged twice with OVA and OVA₃₂₃₋₃₃₉ peptide. Upon the last challenge, tetramer staining was carried out, as previously indicated with minor modifications⁶⁹. Splenocytes were harvested and incubated with a mixture of OVA protein and OVA₃₂₃₋₃₃₉ peptide (1 μ g/mL) with monensin (2 mmol/L; Thermo Fisher Scientific) for 6 h to stimulate antigen-specific T cells. Subsequently, the cells were stained with phycoerythrin-labeled I-Ab OVA₃₂₃₋₃₃₉ tetramer (10 nmol/L) for 1 h at room temperature. After washing, cells were surface stained with an FITC-conjugated anti-CD4 antibody. Then, the cells were fixed, permeabilized, and intracellularly stained with an APC-labeled anti-IL-4 antibody before analysis by flow cytometry.

Histopathological analysis

For histopathological analysis, jejunum and colon tissues were fixed in 4% paraformaldehyde, dehydrated, and embedded in paraffin. The tissues were sectioned into 4- μ m pieces and stained with hematoxylin and eosin (H&E) or Toluidine Blue O for histopathological analysis. The Toluidine Blue O-stained tissues were analyzed for mast cells frequencies by counting the fuchsia spots in each scanned field as previously indicated⁷⁰. Tissue sections were stained and analyzed in a blinded way.

Immunohistochemical and immunofluorescence analyses

Immunohistochemistry (IHC) staining was performed on the above jejunum or colon tissue sections by using primary antibodies of anti-MCC (1:500), anti-MCT (1:500), anti-ZO1 (1:500), anti-Claudin-2 (1:300), and anti-Occludin (1:300), and secondary antibody of HRP goat anti-rabbit IgG (1:200). The IHC sections were pictured on a light microscope (NIKON E100, Japan) and positive area quantified by using ImageJ® software (version 1.53q, National Institutes of Health, Bethesda, MD, USA) as the average optical density.

Immunofluorescence staining was performed on the above colon tissue with primary antibodies of anti-TLR2 (1:1000), anti-TLR4 (1:500), and anti-RAGE (1:500), and secondary antibody of Cy3 goat anti-mouse IgG (1:200). Images were acquired on a Panoramic Scanner (Panoramic DESK, 3DHISTECH) and analyzed by ImageJ® software to determine the relative fluorescence intensity.

Tissue sections were stained and analyzed in a blinded way.

Quantitative real-time RT-PCR

Quantitative RT-PCR was performed by using the Hieff UNICON Universal Blue qPCR SYBR Green Master Mix (Yeasen Bio-Technologies Co., Ltd., Shanghai, China) on a LightCycler 480 II Real-Time PCR System (Roche, Switzerland). Data were normalized to the housekeeping genes of glyceraldehyde-3-phosphate dehydrogenase (GAPDH) and analyzed by the $2^{-\Delta\Delta CT}$ threshold method. The primers sequences (Supplementary Table S5) were designed and synthesized by Sangon Biotech. Co., Ltd. (Shanghai, China).

Taxonomic microbiota analysis

Total genomic DNA was extracted from stool samples by using the CTAB/SDS-based method. The V3–V4 hypervariable regions of the bacterial 16S rRNA gene were amplified with the forward primer 341F (5'-CCTAYGGGRBGCASCAG-3') and reverse primer 806R (5'-GGAC-TACNNGGGTATCTAAT-3'). The purified PCR amplicons were quantified, pooled into equimolar quantities, and sequenced on an Illumina NovaSeq 6000 platform (Novogene Bioinformatics Technology Co., Ltd., Beijing, China) using a 300 bp paired-end model.

Raw sequencing data were processed with the QIIME2 software (Version QIIME2-202006). All Effective Tags were denoised, filtered, and annotated based on the Silva database, and finally clustered into OTUs based on a 97% sequence similarity. The annotated species were generated for abundance and diversity analyses (α -, β -diversity) using QIIME2 software. Significant differences in phylotypes among groups were identified by a taxonomy-based analysis as previously detailed⁷¹.

Cell culture experiments

In vitro mouse BMDC assays. Generation of BMDCs was performed by isolating bone marrow cells from femurs/tibias of BALB/c mice and cultured in conditioned-complete DCs medium with granulocyte-macrophage colony stimulating factor for 6 days as previously reported⁷². To evaluate the effect of BSA-AGE on BMDCs maturation, BMDCs were stimulated with 10 μ g/mL of LPS or 100 μ g/mL of BSA-AGE for 18 h at 37 °C. As reported in a previous study, the concentration of 100–200 μ g/mL represents a physiologically relevant dose of AGEs that human cells may encounter in vivo²⁵. The treated cells were labeled with fluorochrome-conjugated anti-mouse CD11c, CD11b, CD80, CD86, MHC-II and OX40L antibodies. The samples were analyzed by flow cytometry for cell subset proportions as indicated above.

In separate experiments, the effect of BSA-AGE on allergen uptake by BMDCs was evaluated. BMDCs (1×10^5) were pre-treated with 100 μ g/mL of BSA or BSA-AGE for 18 h at 37 °C. Subsequently, FITC-labeled OVA (0.2 mg/mL) was added to the cells, and the uptake of FITC-OVA by BMDCs was assessed at 0 min and 240 min by flow cytometry.

In vitro human PBMC assays. Peripheral blood samples were obtained from 10 healthy volunteers (5 males/5 females; aged 24–25 years, mean 24 ± 0.5 y). The volunteers reported no current or past history of allergic reactions. Informed written consent was obtained from each participant and the study was approved by the Zhejiang Gongshang University Ethics Review Committee (No. 2024030401). Peripheral mononuclear blood cells (PBMCs) were isolated by Ficoll density gradient centrifugation as previously described⁷³. In parallel, a fecal supernatant was prepared from SD- or HAGE-fed mice of the orally sensitized FA model at 12th week (Fig. 2a). The isolated PBMCs were stimulated with 200 μ g/mL of BSA-AGE or 2 mg/mL of fecal supernatant for 48 h 37 °C following previous reports^{25,74}. A BD GolgiStop Protein Transport Inhibitor (containing monensin) was added to the medium (0.07%, v/v) in the last 10 h of cell stimulation. Cells treated with medium alone, non-glycated BSA, or FM-SD served as negative controls. Afterward, the cells were labeled with fluorochrome-conjugated monoclonal antibodies specific for human CD4, IFN- γ , IL-4, RAGE, TLR4, and NF- κ B, and then analyzed by flow

cytometry as described above. In separate experiments, the cells were treated in the absence of the protein transport inhibitor and cell-free supernatants were analyzed for cytokine concentrations using a Bio-Plex Pro Human Cytokine 27-Plex Assay (Bio-Rad, Hercules, CA, USA, #M500KCAFOY-S).

Statistical analysis

Statistical analysis was performed using R 4.0.5 (R Project; www.r-project.org), GraphPad Prism 9.5 (GraphPad Software, La Jolla, CA, USA), and SPSS Statistics 25.0 (IBM, Armonk, NY, USA). Comparisons between two groups were conducted using Student's *t* tests for normally distributed data or Mann–Whitney *U* tests for non-normally distributed data. For comparisons involving three or more groups, one-way ANOVA with Tukey's multiple comparison test was applied to normally distributed data, while Kruskal–Wallis test with Dunn–Bonferroni post hoc analysis was used for non-normally distributed data. Extreme outliers, defined as data points exceeding the 75th percentile plus 1.5 times the interquartile range (IQR) or falling below the 25th percentile minus 1.5 times the IQR, were excluded. Correlation analysis across the data sets was conducted by Spearman correlation analysis. A *p* value less than 0.05 was considered significant. The *p* values were corrected by multiple comparison testing using Benjamini–Hochberg method and presented as *q* values when necessary.

Reporting summary

Further information on research design is available in the Nature Portfolio Reporting Summary linked to this article.

Data availability

The 16S rRNA sequencing data used in this study have been deposited in the NCBI Sequence Read Archive under the accession codes [PRJNA1162303](https://doi.org/10.1038/s41467-025-60235-0), [PRJNA1162283](https://doi.org/10.1038/s41467-025-60235-0), and [PRJNA1162236](https://doi.org/10.1038/s41467-025-60235-0). The mass spectrometry datasets supporting the findings of this study have been uploaded to the Zenodo database under the accession codes [13773165](https://doi.org/10.1038/s41467-025-60235-0) and [13773748](https://doi.org/10.1038/s41467-025-60235-0). All other data generated or analyzed in this study are included in this published article and its Supplementary Information files or are available from the corresponding author on request. Source data are provided with this paper.

References

- Sicherer, S. H. & Sampson, H. A. Food allergy: a review and update on epidemiology, pathogenesis, diagnosis, prevention, and management. *J. Allergy Clin. Immunol.* **141**, 41–58 (2018).
- Loh, W. & Tang, M. L. K. The epidemiology of food allergy in the global context. *Int. J. Environ. Res. Public Health* **15**, 2043 (2018).
- Spolidoro, G. C. I. et al. Frequency of food allergy in Europe: an updated systematic review and meta-analysis. *Allergy* **78**, 351–368 (2023).
- Brough, H. A. et al. Early intervention and prevention of allergic diseases. *Allergy* **77**, 416–441 (2022).
- Lack, G. Update on risk factors for food allergy. *J. Allergy Clin. Immunol.* **129**, 1187–1197 (2012).
- Cabieses, B., Uphoff, E., Pinart, M., Antó, J. M. & Wright, J. A systematic review on the development of asthma and allergic diseases in relation to international immigration: the leading role of the environment confirmed. *PLoS ONE* **9**, e105347 (2014).
- Monteiro, C. A. et al. Ultra-processed foods: what they are and how to identify them. *Public Health Nutr.* **22**, 936–941 (2019).
- Monteiro, C. A., Moubarac, J., Cannon, G., Ng, S. W. & Popkin, B. Ultra-processed products are becoming dominant in the global food system. *Obes. Rev.* **14**, 21–28 (2013).
- Lane, M. M. et al. Ultra-processed food exposure and adverse health outcomes: umbrella review of epidemiological meta-analyses. *BMJ* **384**, e077310 (2024).
- Kong, W., Xie, Y., Zhong, J. & Cao, C. Ultra-processed foods and allergic symptoms among children and adults in the United States: a population-based analysis of NHANES 2005–2006. *Front. Public Health* **10**, 1038141 (2022).
- Kim, Y. H. et al. Maternal perinatal dietary patterns affect food allergy development in susceptible infants. *J. Allergy Clin. Immunol. Pract.* **7**, 2337–2347 (2019).
- Zhang, Q., Wang, Y. & Fu, L. Dietary advanced glycation end-products: perspectives linking food processing with health implications. *Compr. Rev. Food Sci. Food Saf.* **19**, 2559–2587 (2020).
- Nursten, H. E. *The Maillard Reaction: Chemistry, Biochemistry, and Implications* (Royal Society of Chemistry, 2005).
- Scheijen, J. L. J. M. et al. Analysis of advanced glycation end-products in selected food items by ultra-performance liquid chromatography tandem mass spectrometry: presentation of a dietary AGE database. *Food Chem.* **190**, 1145–1150 (2016).
- Zhang, Q. et al. Comprehensive analysis of advanced glycation end-products in commonly consumed foods: presenting a database for dietary AGEs and associated exposure assessment. *Food Sci. Hum. Wellness* **13**, 1917–1928 (2024).
- Uribarri, J. et al. Diet-derived advanced glycation end products are major contributors to the body's AGE pool and induce inflammation in healthy subjects. *Ann. N. Y. Acad. Sci.* **1043**, 461–466 (2005).
- Ott, C. et al. Role of advanced glycation end products in cellular signaling. *Redox Biol.* **2**, 411–429 (2014).
- Zhang, Z. & Li, D. Thermal processing of food reduces gut microbiota diversity of the host and triggers adaptation of the microbiota: evidence from two vertebrates. *Microbiome* **6**, 99 (2018).
- Qu, W. et al. Dietary advanced glycation end products modify gut microbial composition and partially increase colon permeability in rats. *Mol. Nutr. Food Res.* **61**, 1700118 (2017).
- Yu, G. et al. Effects of allergen-specific and non-specific AGEs on the allergenicity of ovalbumin in a mouse model of food allergy. *Mol. Nutr. Food Res.* **67**, 2200221 (2023).
- Body-Malapel, M. et al. The RAGE signaling pathway is involved in intestinal inflammation and represents a promising therapeutic target for Inflammatory Bowel Diseases. *Mucosal Immunol.* **12**, 468–478 (2019).
- Qu, W. et al. Microbiome–metabolomics analysis of the impacts of long-term dietary advanced-glycation-end-product consumption on C57BL/6 mouse fecal microbiota and metabolites. *J. Agric. Food Chem.* **66**, 8864–8875 (2018).
- Yu, W., Freeland, D. M. H. & Nadeau, K. C. Food allergy: immune mechanisms, diagnosis and immunotherapy. *Nat. Rev. Immunol.* **16**, 751–765 (2016).
- Caminero, A., Meisel, M., Jabri, B. & Verdu, E. F. Mechanisms by which gut microorganisms influence food sensitivities. *Nat. Rev. Gastroenterol. Hepatol.* **16**, 7–18 (2019).
- Paparo, L. et al. How dietary advanced glycation end products could facilitate the occurrence of food allergy. *J. Allergy Clin. Immunol.* **153**, 742–758 (2024).
- Levin, M. E. et al. Environmental factors associated with allergy in urban and rural children from the South African Food Allergy (SAFFA) cohort. *J. Allergy Clin. Immunol.* **145**, 415–426 (2020).
- Wang, C. S. et al. Is the consumption of fast foods associated with asthma or other allergic diseases?. *Respirology* **23**, 901–913 (2018).
- Smith, P. K., Masilamani, M., Li, X. & Al, S. E. T. The false alarm hypothesis: food allergy is associated with high dietary advanced glycation end-products and proglycating dietary sugars that mimic alarmins. *J. Allergy Clin. Immunol.* **139**, 429–437 (2016).
- Snelson, M. et al. Processed foods drive intestinal barrier permeability and microvascular diseases. *Sci. Adv.* **7**, eabe4841 (2024).
- Akdis, C. A. Does the epithelial barrier hypothesis explain the increase in allergy, autoimmunity and other chronic conditions?. *Nat. Rev. Immunol.* **21**, 739–751 (2021).

31. Guy, B. The perfect mix: recent progress in adjuvant research. *Nat. Rev. Microbiol.* **5**, 396–397 (2007).
32. Ge, J. et al. Advanced glycosylation end products might promote atherosclerosis through inducing the immune maturation of dendritic cells. *Arterioscler. Thromb. Vasc. Biol.* **25**, 2157–2163 (2005).
33. Adel-Patient, K., Bernard, H., Ah-Leung, S., Créminon, C. & Wal, J.-M. Peanut- and cow's milk-specific IgE, Th2 cells and local anaphylactic reaction are induced in Balb/c mice orally sensitized with cholera toxin. *Allergy* **60**, 658–664 (2005).
34. Eiwegger, T., Hung, L., San Diego, K. E., O'Mahony, L. & Upton, J. Recent developments and highlights in food allergy. *Allergy* **74**, 2355–2367 (2019).
35. Zhang, Q. et al. Early-life risk factors for food allergy: dietary and environmental factors revisited. *Compr. Rev. Food Sci. Food Saf.* **22**, 4355–4377 (2023).
36. Yu, G., He, J., Gao, Z., Fu, L. & Zhang, Q. Protein-bound AGEs derived from methylglyoxal induce pro-inflammatory response and barrier integrity damage in epithelial cells by disrupting the retinol metabolism. *Food Funct.* **15**, 11650–11666 (2024).
37. Liang, Z., Chen, X., Li, L., Li, B. & Yang, Z. The fate of dietary advanced glycation end products in the body: from oral intake to excretion. *Crit. Rev. Food Sci. Nutr.* 1–17 <https://doi.org/10.1080/10408398.2019.1693958> (2019).
38. Huang, Z. et al. Effect of glycation derived from α -dicarbonyl compounds on the in vitro digestibility of ovalbumin: tracing of advanced glycation end-products and immuno-active peptides. *Food Res. Int.* **169**, 112842 (2023).
39. Zhao, D. et al. Digestibility of glyoxal-glycated β -casein and β -lactoglobulin and distribution of peptide-bound advanced glycation end products in gastrointestinal digests. *J. Agric. Food Chem.* **65**, 5778–5788 (2017).
40. Seiquer, I., Rubio, L. A., Peinado, M. J., Delgado-Andrade, C. & Navarro, M. P. Maillard reaction products modulate gut microbiota composition in adolescents. *Mol. Nutr. Food Res.* **58**, 1552–1560 (2014).
41. Kant, R., Blom, J., Palva, A., Siezen, R. J. & de Vos, W. M. Comparative genomics of *Lactobacillus*. *Microb. Biotechnol.* **4**, 323–332 (2011).
42. Bunyavanich, S. et al. Early-life gut microbiome composition and milk allergy resolution. *J. Allergy Clin. Immunol.* **138**, 1122–1130 (2016).
43. Canani, R. B. et al. Effect of *Lactobacillus* GG on tolerance acquisition in infants with cow's milk allergy: a randomized trial. *J. Allergy Clin. Immunol.* **129**, 580–582 (2012).
44. Berin, M. C. & Shreffler, W. G. TH2 adjuvants: implications for food allergy. *J. Allergy Clin. Immunol.* **121**, 1311–1320 (2008).
45. Gold, M. J. et al. Mucosal production of uric acid by airway epithelial cells contributes to particulate matter-induced allergic sensitization. *Mucosal Immunol.* **9**, 809–820 (2016).
46. Ng, N., Lam, D., Paulus, P., Batzer, G. & Horner, A. A. House dust extracts have both TH2 adjuvant and tolerogenic activities. *J. Allergy Clin. Immunol.* **117**, 1074–1081 (2006).
47. Shah, R. R. et al. The development of self-emulsifying oil-in-water emulsion adjuvant and an evaluation of the impact of droplet size on performance. *J. Pharm. Sci.* **104**, 1352–1361 (2015).
48. Hilmenyuk, T. et al. Effects of glycation of the model food allergen ovalbumin on antigen uptake and presentation by human dendritic cells. *Immunology* **129**, 437–445 (2010).
49. Perusko, M. et al. Glycation of the major milk allergen β -lactoglobulin changes its allergenicity by alterations in cellular uptake and degradation. *Mol. Nutr. Food Res.* **62**, 1800341 (2018).
50. Ruiter, B. & Shreffler, W. G. The role of dendritic cells in food allergy. *J. Allergy Clin. Immunol.* **129**, 921–928 (2012).
51. Ullah, M. A. et al. Receptor for advanced glycation end products and its ligand high-mobility group box-1 mediate allergic airway sensitization and airway inflammation. *J. Allergy Clin. Immunol.* **134**, 440–450 (2014).
52. Chen, Y. et al. RAGE ligation affects T cell activation and controls T cell differentiation. *J. Immunol.* **181**, 4272–4278 (2008).
53. Manfredi, A. A. et al. Maturing dendritic cells depend on RAGE for in vivo homing to lymph nodes. *J. Immunol.* **180**, 2270–2275 (2008).
54. Prantner, D., Nallar, S. & Vogel, S. N. The role of RAGE in host pathology and crosstalk between RAGE and TLR4 in innate immune signal transduction pathways. *FASEB J.* **34**, 15659 (2020).
55. Smith, P. K., Venter, C., O'Mahony, L., Canani, R. B. & Lesslar, O. J. L. Do advanced glycation end products contribute to food allergy?. *Front. Allergy* **4**, 1148181 (2023).
56. Basta, G. et al. Advanced glycation end products activate endothelium through signal-transduction receptor RAGE: a mechanism for amplification of inflammatory responses. *Circulation* **105**, 816–822 (2002).
57. Liu, Z. et al. Toll-like receptor 4 plays a key role in advanced glycation end products-induced M1 macrophage polarization. *Biochem. Biophys. Res. Commun.* **531**, 602–608 (2020).
58. Oczypok, E. A. et al. Pulmonary receptor for advanced glycation end-products promotes asthma pathogenesis through IL-33 and accumulation of group 2 innate lymphoid cells. *J. Allergy Clin. Immunol.* **136**, 747–756 (2015).
59. Gangloff, S. C. & Guenounou, M. Toll-like receptors and immune response in allergic disease. *Clin. Rev. Allergy Immunol.* **26**, 115–125 (2004).
60. Steele, E. M. et al. Ultra-processed foods and added sugars in the US diet: evidence from a nationally representative cross-sectional study. *BMJ Open* **6**, e009892 (2016).
61. Maugeri, A. et al. Dietary antioxidant intake decreases carotid intima media thickness in women but not in men: a cross-sectional assessment in the Kardiovize study. *Free Radic. Biol. Med.* **131**, 274–281 (2019).
62. Wright, M. E. et al. Development of a comprehensive dietary antioxidant index and application to lung cancer risk in a cohort of male smokers. *Am. J. Epidemiol.* **160**, 68–76 (2004).
63. McGowan, E. C. & Keet, C. A. Prevalence of self-reported food allergy in the National Health and Nutrition Examination Survey (NHANES) 2007–2010. *J. Allergy Clin. Immunol.* **132**, 1216–1219.e5 (2013).
64. Hussain, M. et al. Basophil-derived IL-4 promotes epicutaneous antigen sensitization concomitant with the development of food allergy. *J. Allergy Clin. Immunol.* **141**, 223–234 (2018).
65. Henle, T. AGEs in foods: do they play a role in uremia?. *Kidney Int.* **63**, S145–S147 (2003).
66. Hussain, M. et al. High dietary fat intake induces a microbiota signature that promotes food allergy. *J. Allergy Clin. Immunol.* **144**, 157–170 (2019).
67. Neeland, M. R. et al. Mass cytometry reveals cellular fingerprint associated with IgE+ peanut tolerance and allergy in early life. *Nat. Commun.* **11**, 1–10 (2020).
68. Globig, A. M. et al. High-dimensional profiling reveals Tc17 cell enrichment in active Crohn's disease and identifies a potentially targetable signature. *Nat. Commun.* **13**, 3688 (2022).
69. Zeng, W. et al. Staphylococcal enterotoxin A-activated regulatory T cells promote allergen-specific TH2 response to intratracheal allergen inoculation. *J. Allergy Clin. Immunol.* **139**, 508–518.e4 (2017).
70. Abdel-Gadir, A. et al. Microbiota therapy acts via a regulatory T cell MyD88/ROR γ t pathway to suppress food allergy. *Nat. Med.* **25**, 1164–1174 (2019).
71. Wang, Y. et al. Variations in oral microbiota and salivary proteomics reveal distinct patterns in polysensitized individuals. *Allergy* **77**, 1899–1902 (2022).
72. Zhou, Y. et al. Secretions from hypochlorous acid-treated tumor cells delivered in a melittin hydrogel potentiate cancer immunotherapy. *Bioact. Mater.* **9**, 541–553 (2022).
73. De Filippis, F. et al. Specific gut microbiome signatures and the associated pro-inflammatory functions are linked to pediatric allergy and acquisition of immune tolerance. *Nat. Commun.* **12**, 1–11 (2021).

74. Behary, J. et al. Gut microbiota impact on the peripheral immune response in non-alcoholic fatty liver disease related hepatocellular carcinoma. *Nat. Commun.* **12**, 187 (2021).

Acknowledgements

This study was supported by the State key research and development plan (No. 2024YFF1105900, L.L.F. and Q.Z.Z.), the Zhejiang Provincial Natural Science Foundation of China (grant LZ23C200001, L.L.F.) and the Natural Science Foundation of China (grant 32202202, Q.Z.Z.).

Author contributions

Conceptualization: Q.Z.Z. and L.L.F.; methodology: Q.Z.Z., G.Y., Y.H.J., X.R.Y., and C.W.; investigation: Q.Z.Z., G.Y., Y.H.J., Q.Q.L., and H.T.L.; writing—original draft: Q.Z.Z., G.Y., and Y.H.J.; writing—review & editing: Q.Z.Z. and L.L.F.; source: H.N.S., Z.S.G., Q.Q.W., and J.L.S.; project administration: L.L.F.; funding acquisition: Q.Z.Z. and L.L.F.

Competing interests

The authors declare no competing interests.

Additional information

Supplementary information The online version contains supplementary material available at <https://doi.org/10.1038/s41467-025-60235-0>.

Correspondence and requests for materials should be addressed to Linglin Fu.

Peer review information *Nature Communications* thanks Peter K. Smith, Linette EM Willemsen and the other, anonymous, reviewer(s) for their contribution to the peer review of this work. A peer review file is available.

Reprints and permissions information is available at <http://www.nature.com/reprints>

Publisher's note Springer Nature remains neutral with regard to jurisdictional claims in published maps and institutional affiliations.

Open Access This article is licensed under a Creative Commons Attribution-NonCommercial-NoDerivatives 4.0 International License, which permits any non-commercial use, sharing, distribution and reproduction in any medium or format, as long as you give appropriate credit to the original author(s) and the source, provide a link to the Creative Commons licence, and indicate if you modified the licensed material. You do not have permission under this licence to share adapted material derived from this article or parts of it. The images or other third party material in this article are included in the article's Creative Commons licence, unless indicated otherwise in a credit line to the material. If material is not included in the article's Creative Commons licence and your intended use is not permitted by statutory regulation or exceeds the permitted use, you will need to obtain permission directly from the copyright holder. To view a copy of this licence, visit <http://creativecommons.org/licenses/by-nc-nd/4.0/>.

© The Author(s) 2025